Study on High Performance Lignin/Natural Rubber Bionanocomposites

PHAKKEEREE TREETHIP

Kyoto Institute of Technology

CONTENTS

	Page
GENERAL INTRODUCTION	1
References	12
CHAPTER 1 Lignin as effective reinforcing filler in natural rubber	16
1.1 Introduction	17
1.2 Experimental	18
1.2.1 Materials	18
1.2.2 Tensile measurements	20
1.2.3 Laser scanning confocal microscopy measurement	20
1.2.4 Transmission electron microscopy measurement	20
1.2.5 Scanning probe microscopy measurement	21
1.3 Results and discussion	21
1.3.1 Tensile characteristics of lignin/NR biocomposite prepared by soft processing method	21
1.3.2 Morphology observations of lignin/NR biocomposite	23
1.4 Conclusions	28
References	28
CHAPTER 2 Effect of Lignin Content on Mechanical Properties of Lignin/Natural Rubber Soft Biocomposites	31
2.1 Introduction	32
2.2 Experimental	33
2.2.1 Materials	33
2.2.2. Raman spectroscopy	34
2.2.3 Tensile measurements	35
2.2.4 Measurement of network-chain density	36
2.2.5 Morphology observations by laser scanning confocal microscopy and scanning probe microscopy	36
2.2.6 Evaluation of Payne effect	36
2.2.7 Dynamic mechanical analysis	37
2.3 Results and discussion	37
2.3.1 Tensile properties of lignin filled NR biocomposites	37

CONTENTS (cont.)

	Page
2.3.2 Morphological characteristics of lignin/NR soft biocomposites	41
2.3.3 Mechanical properties of lignin/NR soft biocomposites	47
2.4 Conclusions	50
References	51
CHAPTER 3 Strain-Induced Crystallization Behaviours of Lignin/Natural Rubber Soft Biocomposites	54
3.1 Introduction	55
3.2 Experimental	57
3.2.1 Materials	57
3.2.2. Morphology observation by scanning probe microscopy	58
3.2.3 Quick time-resolved simultaneous wide-angle X-ray diffraction and tensile measurements	58
3.2.4 WAXD analysis	60
3.3 Results and discussion	63
3.3.1 Characteristic of strain-generated crystallites in lignin/NR soft biocomposites	63
3.3.2 Relationship between tensile properties and SIC behaviours of lignin/NR soft biocomposites	72
3.4 Conclusions	74
References	75
SUMMARY	78
LIST OF PUBLICATIONS	81
ACKNOWLEDGEMENTS	82

GENERAL INTRODUCTION

General introduction

Rubber can be classified into two main categories, i.e., natural rubber (NR) and synthetic rubber. NR is the only one biomass among many kinds of rubbers with unique chemical and physical properties, especially highly elastic property, which cannot be mimicked by synthetic rubbers, due to entropy has been notable [1-3]. It is well known that *Hevea brasiliensis* is an outstanding commercial source of NR, which has been utilized in rubber industry. The origin of the *Hevea brasiliensis* was around the basin of Amazon river, and it was distributed to other tropical regions in later part of 19^{th} century [1-3]. Commonly, NR latex is a sap of *Hevea brasiliensis* tree (Figure 1). However, the most practical source of NR for rubber manufactures is solid NR due to the limitation of NR latex in many ways, for example, inability of NR lattices against coagulation [4,5]. This trouble was solved by Norris [6] and Johnson [7], they found that NR latex can be preserved by using ammonia. Since then ammonia has come to be regarded as the standard preservation for NR latex [5], it was possible to be distributed to customers in many regions. Nowadays, several kinds of NR latexes are available, such as high ammonia latex (HA), low ammonia latex, deproteinized latex, and compounded prevulcanized latex. These concentrated NR latexes are marketed for producing various specific products. For example, deproteinized latex is generally used to manufacture medical gloves for surgical operations in order to minimize the allergic response to the patients and the medical staffs [8]. Among them, HA is the most widely used latex due to its higher mechanical stability than the others.

It is well known that NR has excellent green strength comparing to synthetic rubber, this is one of unique properties in NR. However, this strength does not strong enough

Figure 1 Natural rubber latex from *Hevea brasiliensis* tree.

and it is unstable. Thus, in most practical applications, NR is mixed with a variety of compounding ingredients such as cross-linking reagents for formation of network structure, fillers for improvement of practical mechanical properties, various kinds of stabilizers for improvement of poor resistance against oxidation, and processing aids for good processability in manufacturing. Improvement of mechanical properties by mixing filler has been done for a long time. The fillers are classified into two main groups, which are carbon black (CB) and non-carbon black fillers. The former is still much more important than all the others. NR/CB nanocomposites were on the market well before that of the fiber-reinforced plastics (FRPs), and long before the time when the word "nanotechnology" was coined and came onstage. The NR/CB composites are reasonably proved to be the so-called "precursor of composites", or historically the first commercial product of nanotechnology. The reinforcement of active fillers has been believed that the diameter of fillers (usually assumed to be spherical) should be as small as possible. However, it is also known that nanometer (nm) size fillers, such as CBs are

subjected to cluster formation leading to so-called “structure” in the rubbery matrix. The “structure” was known very early, and it has popularly been believed that to disperse each of the nanoparticles homogeneously in the rubber matrix should be the most favorable dispersion for rubber reinforcement. Ideally, one particulate nanofiller, CB is displayed in which the surface is encircled by a rubbery layer as shown in Figure 2A. Rubber in the layer has been well recognized among rubber chemists and technologists as “bound rubber” [9]. In particular, CB particles are associated during their industrial manufacturing process due to so-called filler-filler interaction (quantum mechanical dispersion force, i.e., the van der Waals force is considered here) and the resulting CB aggregate is encircled by the bound rubber during the mechanical mixing into rubbery matrix as shown in Figure 2B. The aggregate formation is due to the filler’s huge surface area of the nm size. Hence, the interaction between fillers is reasonably assumed to be larger than the filler-rubber interaction.

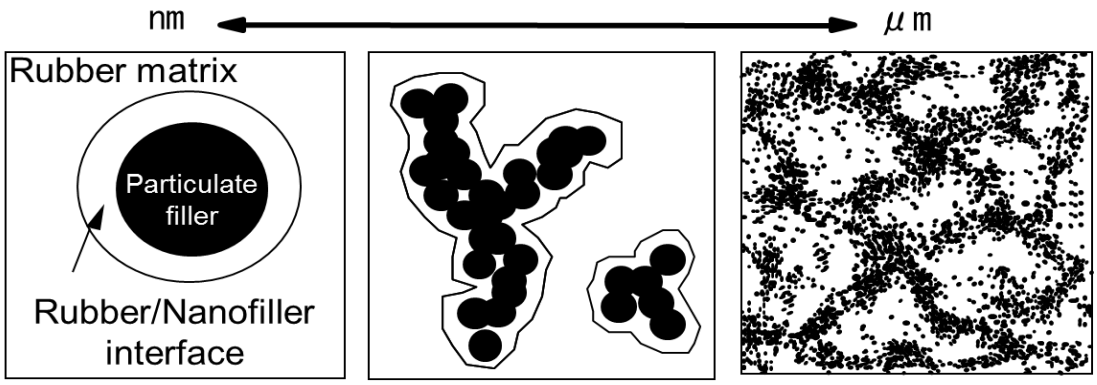

Figure 2 Schematic representation of nanofiller morphology in the rubbery matrix. (A) Particulate filler size from *ca.* 3 to 100 nm. (B) Aggregate size from *ca.* 20 to 1000 nm. (C) Agglomerate size from *ca.* 1000 nm to 1000 μm [10].

The agglomerate, i.e., the cluster of aggregates, may often be a pseudo network structure as suggested in Figure 2C. Note that both aggregate and agglomerate are so-called van der Waals cluster, and even the agglomerates are encircled by the bound rubber layers in the rubbery matrix. Until recently, "The better the dispersion, the greater the reinforcement" has been a popular belief among some rubber technologists. Not the highest dispersion, i.e., complete isolation of each particle, but achieving a certain dispersion that may be favorable to form a network-like structure of nanofiller as shown in Figure 2C is the best dispersion, in terms of rubber reinforcement.

Nowadays, however, the rubber technologists are much more interested in the non-carbon black fillers than before. CBs are produced from petroleum which is supposed to be exhausting, and are not assumed to be sustainable. Therefore, particulate silica has been focused from some time ago to manufacture so called "green tires" [11-13]. Beside silica, various biopolymers or natural plant products such as starch, cellulose, rubber leaf, pineapple leaf, bamboo leaf, sedge, sugar cane, jute, tapioca, and others are to be considered, and some have been tested as a filler for rubbers [14,15]. These fillers are expected to be eco-friendly, competitive in terms of cost, and applicable to lots of end uses for both industrial and everyday articles [16,17]. Recently, the bio-based composites become more popular, because they are renewable, environmental friendly and sustainable, and may possibly contribute to the decrease of carbon dioxide emission against the global warming. Therefore, many researchers studied on the preparation of bio-based composites. One of interested bio-based composites is NR/biofillers. The biofillers such as oil palm fibers, pineapple leaf fibers, lignin, etc., have been used to blend with NR in order to improve mechanical properties, to reduce the cost and to obtain ecological friendly materials [14,15,18-20]. Among

biofillers, lignin has been targeted to be reinforcing filler for NR as reported in review papers [19,20]. Unlike CB which is a petrochemical product, lignin, a natural polymer and one of the main components of wood [21,22], thus is being preferred from the sustainable development (SD) point of view. Typically, lignin is an amorphous natural polymer, occurs in woods and it is the second most abundant biopolymer next to cellulose. It prevents wood from mechanical and biological stresses. Lignins vary in structure according to their method of isolation and their plant source. Lignin is generated during kraft pulping of paper manufacturing in alkaline medium, namely, kraft lignin. By using kraft process or sulfate process, an aliphatic sulfonic acid (SO_3H) becomes a part of the lignin backbone in the presence of a suitable counter ion, for example, Na, Ca, Mg, NH_4, etc. In addition, kraft lignins are water-insoluble and solvent-insoluble products that dissolve in the alkali due to its high concentration of phenolic hydroxyl groups [21,23,24]. As mentioned above, the incorporation of lignin into different polymer materials has been stronger focused because of some properties, such as reinforcing effect, strong intramolecular interactions, processing ability, stabilizing effect, and biodegradability [25]. Many efforts have been paid to the effective utilization of the lignin waste [19,20,26]. However, an adequate method to use lignin as effective reinforcing filler for rubber did not achieve until now. For example, nanocomposites using nanolignin and natural rubber were also prepared [26]. The nanocomposites were prepared using co-precipitation of colloidal lignin−cationic polyelectrolyte complexes and rubber latex. The nanolignin was synthesized by fabricating colloidal lignin-poly(diallyldimethylammonium chloride) (PDADMAC) complexes (LPCs) employing the self-assembly technology. However, this technique seem to complicate and the mechanical properties did not improve so much.

One of possible reasons that inadequate method for preparing NR/lignin composites is its poor processability by conventional mixing method. By this method, the composites were prepared by mechanical mixing and followed by heat molding under pressure. Hence, the incorporation of filler to rubber and fine dispersion of filler have been considered that difficult to achieve. According to disadvantages of conventional mixing method, another methods to improve those disadvantage points have been researched. Soft processing would be regarded as one of the possible techniques to achieve a good dispersion state of nanofiller. The premise of excellent reinforcement of rubber composites, where very fine filler particles, usually nanofillers, are organized into a network-like morphology in the rubber matrix similarly as shown in Figure 2C. The words “soft processing method” are used for the procedures carried out through a liquid state (not involving a solid state), where rubber latex can conveniently be used as a source material. The manufacturing of soft composites by the soft process is generally started by adding a liquid state precursor of filler or filler solution into the latex. Before the addition, it is necessary to check the colloidal stability of the mixture to avoid coagulation. Then, the effect of the mixing of suitable cross-linking reagents is checked. The modification of the recipe for vulcanization may be sometimes needed in order to maintain the colloidal stability during the processing. After all reagents are mixed into the latex, the mixture of the liquid state is subjected to casting onto a clean flat plate maintained horizontally in order to form a film. Although a dipping technique into the latex mixture may be of use for a tube or some other shaped films, it may be recommended only when such a specific shape is necessary in the industrial manufacturing.

By using this soft process, recently, our research group has successfully prepared *in*

situ silica filled NR composites (*in situ* silica/NR) with high performance mechanical properties. The *in situ* silica/NR composite did show a network-like or biphasic structured morphology, which is shown in Figure 3 as observed by scanning probe microscopy (SPM) [27]. Two samples having different silica contents of 10 phr and 17 phr generated in NR matrix are abbreviated to Si10 and Si17, respectively. In the phase images, bright and dark phases are attributed to hard and soft phases which are silica and rubber phases, respectively. It can be seen that around rubber particles, particulate

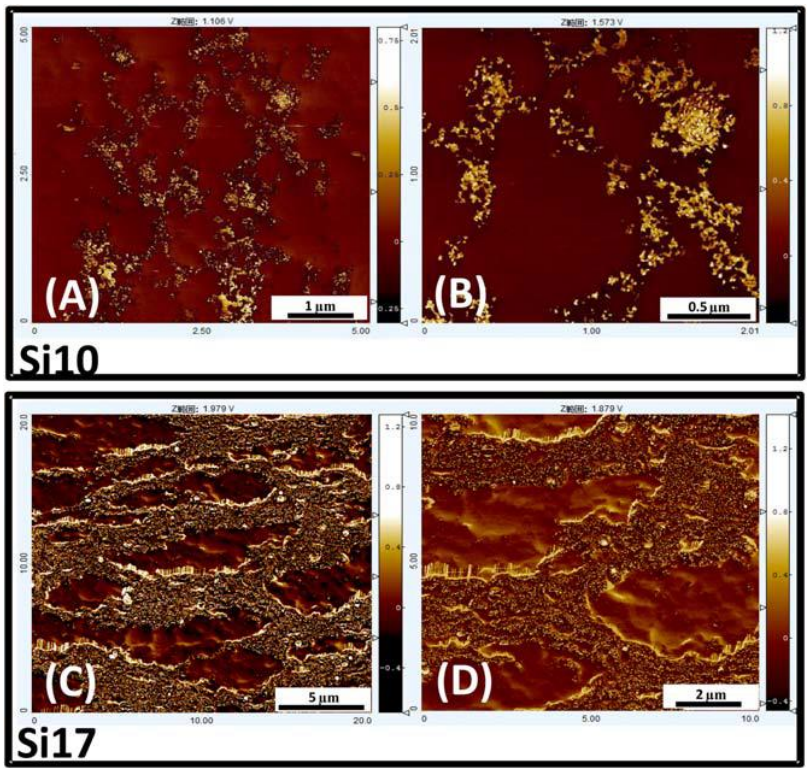

Figure 3 SPM photographs of *in situ* silica filled peroxide cross-linked nanocomposites. Upper and lower images show Samples Si10 and Si17, respectively. (A), (B), (C), and (D) were observed at the magnifications of 25 μm^2, 4 μm^2, 400 μm^2, and 100 μm^2, respectively [27].

silica was generated to form bilayer structure composites of NR matrix and silica layers. This specific silica phase may be regarded as a good model of filler network, which is the origin of the reinforcement effect by this filler [27]. Thus, the soft processing technique is found to be very useful for preparing NR nanocomposites of a network-like state of the contained nanofiller. This technique can be recognized to be importance not only for academic study but also for industrial manufacturing of soft nanocomposites. Accordingly, this process was greatly applied for the lignin/NR soft nanobiocomposites in this present study. When NR is used as the matrix, the lignin/NR biocomposite which is a favorable material from the SD standpoint since the product is carbon-neutral.

One of the remarkable properties of NR is strain-induced crystallization (SIC): NR can be crystallized under stretching, for example, resulting in high green strength in gum NR. Typically, NR is an amorphous at room temperature, however it is crystallizable upon stretching, which has been accepted to be one of the factors for high performance of NR. In 1925, Katz firstly reported the SIC behaviour of vulcanized and unvulcanized NR using X-ray diffraction. In addition, unstrained NR also crystallizable under cooling state, this phenomenon is called as thermally induced crystallization or cold crystallization which was studied by Bekkedahl and Wood around in 1940 [28,29]. However, until recently, the SIC behaviour of NR has been extensively studied [30-41]. SIC phenomena can be explained as following (Figure 4): Before stretching as seen in Figure 4A, cross-links are distributed uniformly for easier understanding. After deformation as shown in Figure 4B, short chains are fully stretched. Note that the distribution of cross-links is no longer uniform to keep many network chains in the random-coil-like state. The fully stretched chains act as nucleus of crystallites (yellow parts) as shown in Figure 4C. Thus, the NR crystallites are usually observed to grow up

(A) (B) (C)

Figure 4 Model of nucleation and crystallization in vulcanized NR [38].

in the direction perpendicular to the molecular chain axis [38-43].

The new soft process for manufacturing the lignin/NR biocomposites from NR latex: Lignin was dissolved in an alkaline water, and mixing of the lignin *aq.* solution with NR latex gave a liquid mixture of lignin and NR. The evaporation afforded a soft composite film, which was prepared without any solid-state mechanical mixing at all [44]. The author has success to prepare these samples during her master course at Mahidol University. Additionally, the lignin/NR biocomposites exhibited fine dispersion of lignin in rubber matrix and high mechanical properties. Thus, in the present study, the lignin/NR soft biocomposites were further investigated the relationship between morphology and mechanical properties. Some characteristics to endow the mechanical properties would be elucidated in this study by conducting SIC

analyses. The study can be divided into three chapters as follows;

In Chapter 1, the relationship between morphology and mechanical properties of the lignin/NR biocomposite was revealed, where the sample was prepared by using NR latex and 10 parts per one hundred rubber by weight of sodium lignosulfonate, namely, the soft processing method. A morphological feature of the lignin/NR biocomposite was found to be an origin of high performance mechanical properties. The formation of network-like structure of lignin was proposed to be a key to produce high performance lignin/NR biocomposites.

In Chapter 2, an effect of lignin contents on the morphology of the lignin/NR soft biocomposites was elucidated by addition of 5, 10, 20 and 40 phr lignin using the soft process. The formation of network-like structure of different amounts of lignin was investigated and discussed relating to their mechanical properties.

In the last chapter, Chapter 3, the effect of specific morphology on SIC behaviour of the lignin/NR soft biocomposites was disclosed. As mentioned above, SIC behaviour is an outstanding property of NR. Therefore, the effect of lignin contents on the SIC behaviour was studied for the lignin/NR soft biocomposites by using simultaneous time-resolved wide-angle X-ray diffraction and tensile measurements. Especially, the role of network-like structure of lignin on the SIC behaviour was discussed.

On the basis of the contents in three chapters, this thesis introduces an intrinsic morphology of biocomposites which prepared by using NR latex and *aq.* sodium lignosulfonate. By using the soft process, the NR particles in NR latex also act as templates in the case of lignin filling NR. The obtained network-like structure of lignin clearly resulted in the enhancement mechanical properties, which will give an important hint to analyze the role of CB filler network in the rubber products. Therefore, the

author wishes that this thesis would be useful for development of natural rubber biocomposites technology.

References

1. L. Bateman, *The chemistry and physics of rubber-like substances*, Maclaren & Sons, London, 1963, 301.

2. A. D. Roberts, *Natural rubber science and technology*, Oxford Science Publications, Oxford, 1988, 177.

3. S. Kohjiya, *Natural rubber: from the odyssey of the Hevea tree to the age of transportation*, Smithers RAPRA, Shrewsbury, 2015.

4. D. C. Blackley, *Polymer lattices science and technology*, Volume 1, Chapman & Hall, London, 1997.

5. D. C. Blackley, *Polymer lattices science and technology*, Volume 2, Chapman & Hall, London, 1997.

6. H. L. Norris, S. T. Armstrong, United States Patent No. 9, 891, 26 July, 1853.

7. W. Johnson, British Patent No. 467, 18 August, 1953.

8. T. Palosuo, *Chemistry, manufacturing and applications of natural rubber*, eds S. Kohjiya, Y. Ikeda, Cambridge, Woodhead/Elsevier, 2014, Ch. 18, pp. 452-482.

9. G. Kraus, *Reinforcement of elastomers*, New York: Interscience; 1956.

10. S. Kohjiya, A. Kato, T. Suda, J. Shimanuki, Y. Ikeda, *Polymer*, 2006, **47**, 3298.

11. R. Rauline, *(to La Compagnie Generale des Etablissements Michelin*), EP 0501227A1. February 12 (1992).

12. S. Kohjiya, A. Kato, Y. Ikeda, *Prog. Polym. Sci.*, 2008, **33**, 979-997.

13. Y. Shinohara, H. Kishimoto, K. Inoue, Y. Suzuki, A. Takeuchi, K. Uesugi, N. Yagi,

K. Muraoka, T. Mizoguchi, Y. Amemiya, *J. Appl. Cryst.*, 2007, **40**, s397–s401.

14. G. Bogoeva-Gaceva, M. Avella, M. Malinconico, A. Buzarovska, A. Grozdanov, G. Gentile, M. E. Errico, *Polym. Compos.*, 2007, **28**, 98-107.

15. R. P. Kumar, K. C. M. Nair, S. Thomas, S. C. Schit, K. Ramamurthy, *Comp. Sci. and Tech.*, 2000, **60**, 1737-1751.

16. B. Kosikova, A. Gregorova, A. Osvald, J. Krajcovicova, J. Appl. Polym. Sci., 2007, **103**, 1226- 1231.

17. C. Nakason, A. Kaesman, S. Homin, S. Kiatkamjomwong, *J. Appl. Sci*., 2001, **81**, 2803.

18. M. S. Sreekala, M. G. Kumaran, S. Thomas, *J. Appl. Polym. Sci*., 1997, **66**, 821.

19. V. K. Thakur, M. K. Thakur, P. Raghavan, M. R. Kessler, *ACS Sustainable Chem. Eng.*, 2014, **2**, 1072.

20. E. Ten, W. Vermerris, *J. Appl. Polym. Sci.*, 2015, **132**, 42069(1).

21. W. G. Glasser, S. Sarkanen, *Lignin: properties and materials, ACS Symposium Series 397*, American Chemical Society, Washington DC, 1989.

22. E. A. MacGregor, C. T. Greenwood, *Rubber and lignin. Polymer in nature. Chichester*, John Wiley & Sons, 1980.

23. J. H. Lora, W. G. Glasser, *J. Polym. Environ.*, 2002, **10**, 39.

24. J. Huang, L. Zhang, H. Wei, X. D. Cao, *J. Appl. Polym. Sci.*, 2004, **93**, 624.

25. A. Gregoroúa, B. Košíková, R. Moravčík, *Polym. Degrad. Stab.*, 2006, **91**, 229.

26. C. Jiang, H. He, H. Jiang, L. Ma, D. M. Jia, *eXPRESS Polymer Letters*, 2013, **7**, 480.

27. A. Tohsan, R. Kishi, Y. Ikeda, *Colloid Polym. Sci.*, 2015, **293**, 2083.

28. N. Bekkedahl, L. A. Wood, *Ind. Eng. Chem.*, 1941, **33**, 381.

29. L. A. Wood, N. Bekkedahl, *J. Appl. Phys.*, 1946, **17**, 362.

30. J. R. Katz, *Naturwiss*, 1925, **19**, 410.

31. P. J. Flory, *Principles of polymer chemistry*, Cornell University, Ithaca, 1953.

32. L. R. G. Treloar, *The physics of rubber elasticity*, Clarendon Press, Oxford, 1975.

33. G. R. Mitchell, *Polymer*, 1984, **25**, 1562.

34. L. Mandelken, *Crystallization of polymers, vol 1: equilibrium concepts*, 2nd ed., Cambridge University Press, Cambridge, 2002.

35. M. Tsuji, S. Kohjiya, *Prog Polym Sci*, 1995, **20**, 259.

36. S. Murakami, K. Senoo, S. Toki, S. Kohjiya, *Polymer*, 2002, **43**, 2117.

37. S. Toki, I. Sics, S. Ran, L. Liu, B. S. Hsiao, S. Murakami, K. Senoo, S. Kohjiya, *Macromolecules*, 2002, **35**, 6578.

38. M. Tosaka, S. Murakami, S. Poompradub, S. Kohjiya, Y. Ikeda, S. Toki, I. Sics, B. S. Hsiao, *Macromolecules*, 2004, **37**, 3299.

39. M. Tosaka, S. Kohjiya, S. Murakami, S. Poompradub, Y. Ikeda, S. Toki, I. Sics, B. S. Hsiao, *Rubber Chem Technol*, 2004, **77**, 711.

40. Y. Ikeda, Y. Yasuda, S. Makino, S. Yamamoto, M. Tosaka, K. Senoo, S. Kohjiya, *Polymer*, 2007, **48**, 1171.

41. Y. Ikeda, Y. Yasuda, K. Hijikata, M. Tosaka, S. Kohjiya, *Macromolecules*, 2008, **41**, 5876.

42. J. Che, S. Toki, J. L. Valentin, J. Brasero, A. Nimpaiboon, L. Rong, B. S. Hsiao, *Macromolecules*, 2012, **45**, 6491.

43. S. Toki, C. Burger, B. S. Hsiao, S. Amnuaypornsri, J. Sakdapipanich, Y. Tanaka, *J. Appl. Polym. Sci.: Part B: Polym. Phys.*, 2008, **46**, 2456.

44. T. Phakkeeree, *Preparation, structure, and properties of natural rubber/lignin*

nanocomposites, Master thesis of Mahidol University, 2009.

CHAPTER 1

CHAPTER 1

Lignin as Effective Reinforcing Filler in Natural Rubber

1.1 Introduction

Natural rubber (NR) is an important industrial material, such as in tyre manufacturing due to its excellent elastic modulus, tensile strength, tear strength, etc. [1,2]. As mentioned previously in the general introduction, a promising reuse of the lignin waste, e.g. sodium lignosulfonate, trials of the use of lignin wastes as a filler component in rubbery composites have also been carried out extensively [3-11]. However, adequate techniques to obtain high performance NR biocomposites have been not established yet [3-11]. The NR biocomposites from lignin filled NR latex (lignin/NR biocomposites) is focused in this study. The study on preparation of lignin/NR biocomposites by using *aq.* sodium lignosulfonate and NR latex was conducted previously [12]. In the previous study, preparation technique to obtain high performance lignin/NR biocomposites was established [12]. Additionally, the film formation for the lignin/NR biocomposites was provided in order to retain a fine dispersion of lignin and to attain specific morphology similarly to *in situ* silica/NR composites [13,14]. By using this preparation method, the lignin/NR biocomposites supposed to exhibit high mechanical properties. However, relationship between mechanical properties and morphological features has still been unclear.

Therefore, in present study, the lignin/NR biocomposites have been further elucidated the relationship between mechanical properties and morphological features. A characteristic of morphology was revealed to have affected to enhance mechanical

properties which can be obtained by using transmission electron microscopy photographs and scanning probe microscopy images. Accordingly, an alternative useful morphological effect of lignin to significantly reinforce the lignin/NR biocomposite was reported for the first time. The obtained results also provide new insights into the reinforcement mechanism of rubber by filler filling in the case of organic filler for a greater sustainable materials nowadays.

1.2. Experimental

1.2.1 Materials

The lignin/NR soft biocomposites, which were prepared by the soft processing method, were used [12]. Lignin used in this study was commercial sodium lignosulfonate (Pearllex NP, Nippon Paper Chemicals, Co., Ltd., Japan). It was a powder and classified as a high molecular weight grade [15]. The content of sulfonate group was 1.8 mmol/g.

The sodium lignosulfonate was dissolved in 0.1 M aqueous NaOH. The final concentration of the lignin solution was 30 w/v%. A lignin/NR soft biocomposite film was prepared by mixing with sulfur cross-linking reagents and followed by mixing with 20 mL of the lignin aqueous solution to give a liquid mixture of lignin/NR. In the other word, in this study, 10 phr lignin was added to the NR latex for the preparation of lignin/NR soft biocomposite, here, the abbreviation of composite is NR-L10-S-soft. The evaporation on a glass plate at r.t. for a few days afforded a soft composite film. Then, the film was subjected to cross-linking at 70 °C for 4 h and dried at r.t. under a reduced pressure. An unfilled sample (NR-L0-S-soft) was also prepared by the same method. The schematic for the soft processing method is shown in Figure 1.1.

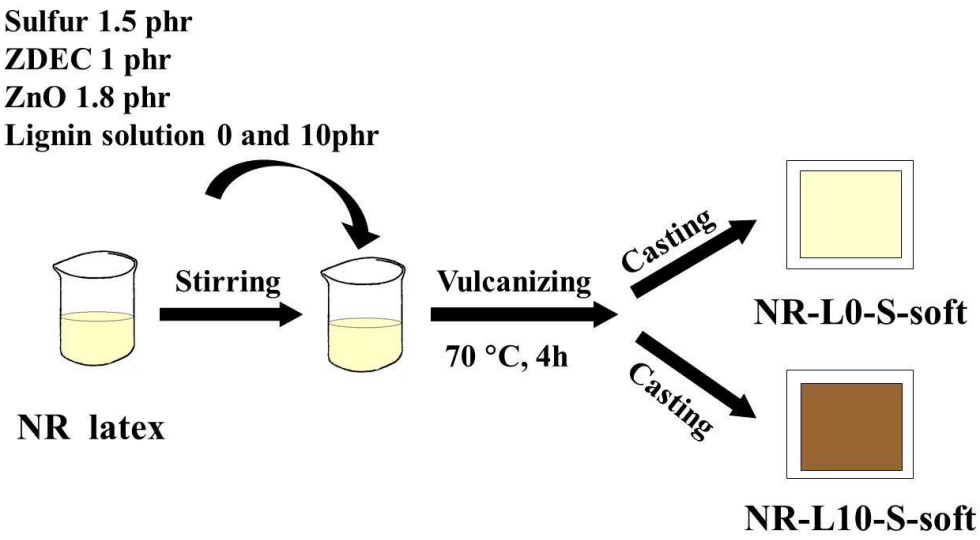

Figure 1.1 **S**chematic for the soft processing method.

As reference samples, lignin/NR biocomposites were also prepared from solid NR and the lignin powder by milling, i.e., mechanical mixing on a two-roll mill at r.t. Solid NR (RSS no.1) was mixed with 10 phr lignin, 1.0 phr ZnO, 2.0 phr stearic acid, 1.0 phr *N*-cyclohexyl-2-benzothiazole sulfonamide (CBS) and 1.5 phr sulfur for sulfur cross-linking. Unfilled sulfur cross-linked sample was also prepared by conventional mixing using the same recipe. Peroxide cross-linked composites were also prepared, where 10 phr lignin and 1.0 phr dicumyl peroxide were mixed with solid NR or isoprene rubber (IR) on the two-roll mill. The rubber compounds were molded into a sheet of 1 mm thickness by heat pressing at 140 °C for 12 min and 155 °C for 30 min for sulfur cross-linking and peroxide cross-linking, respectively. The biocomposites containing lignin with 0 and 10 phr are abbreviated as NR-L0-S-mill, NR-L10-S-mill, NR-L10-P-mill and IR-L10-P-mill. In the sample codes, “L”, “number”, “S” and “P”

mean lignin, a lignin content in phr, sulfur cross-linking and peroxide cross-linking, respectively.

1.2.2 Tensile measurements

Tensile properties were measured at r.t. using a tailor-made tensile tester (ISUT-2201, Aiesu Giken, Co., Japan). Outside and inside diameters of ring-shaped samples were 13.7 and 11.7 mm, respectively. They were stretched up at a stretching speed of 100 mm/min, i.e., the strain speed was about 4.98 per min. A stretching ratio (α) is defined as "$\alpha = l/l_0$", where l is a length after deformation, and l_0 is an initial length, respectively.

1.2.3 Laser scanning confocal microscopy measurement

Laser scanning confocal microscopy (LSCM) was conducted using a Nikon Laser Scanning Confocal Microscope System A1R with a 20× objective (numerical aperture = 0.75, CFI Plan Apochromat 20×/0.75 DIC M, Nikon Co., Japan) at r.t. The laser wavelength was 488 nm. The schematic of LSCM is shown in Figure 1.2.

1.2.4 Transmission electron microscopy measurement

Transmission electron microscopy (TEM) was then conducted for NR-L10-S-soft using a transmission electron microscope (JEOL TEM-100U) without staining the specimen. The accelerating voltage was 80 kV. An ultra thin film specimen was prepared by using a MT-XL Ultra-microtome (Boeckeler Instrument, Inc.) in a mixture solvents of ethylene glycol and ethanol (50% by volume).

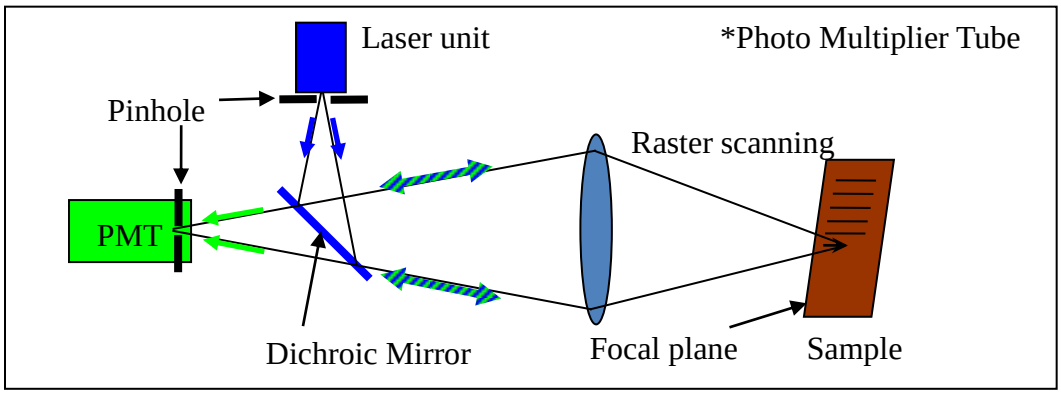

Figure 1.2 Schematic diagram of laser scanning confocal microscope.

1.2.5 Scanning probe microscopy measurement

Scanning probe microscopy (SPM) observation was performed using a Bruker AXS Nanoscope III a plus D3100 (Bruker Co.) at r.t. The probes were OMCL-AC160TS (Olympus Co.). The surface of sample was prepared by cutting using an ultra-microtome (LEICA, UC6) at -100 °C.

1.3. Results and discussion

1.3.1 Tensile characteristics of lignin/NR biocomposite prepared by soft processing method

Figure 1.3 shows stress-strain curves of the 10 phr lignin filled composites with the unfilled samples. It was found that the biocomposite prepared by the soft processing method showed the largest stresses up to the high strain among the samples. This phenomenon ascribed to the reinforcement effect of lignin to NR. Additionally, 10 phr lignin filled NR prepared by this processing method, i.e., NR-L10-S-soft, exhibited the abrupt increasing of tensile stress at $1 \leq \alpha \leq 2$, which suggested the filler-filler

interaction. Meanwhile, the others samples did not show this behaviour, on the other hand, NR-L10-S-soft probably contained filler network. It should be noted that only 10 phr filling of lignin significantly enhanced the tensile properties of the biocomposite, NR-L10-S-soft. For example, the stress at stretching ratio (α) = 8 of NR-L10-S-soft was high, more than double that of NR-L10-S-mill.

When conventional milling was used, the stress of 10 phr lignin filling sample was slightly increased, similar to that of the CB system. Even when the peroxide cross-linking was used to prepare the lignin-filled rubbers, good reinforcement was not achieved. It is to be noted that the conventional mixing method cannot provide good reinforcement by the addition of lignin for both cross-link systems, on the other hand, the reinforcing effect by lignin did not promote not only for NR but also synthetic isoprene rubber (IR), as shown by NR-L10-P-mill and IR-L10-P-mill, respectively. NR-L10-P-mill showed very similar stress-strain curve to IR-L10-P-mill and both samples exhibited lower tensile properties than NR-L10-S-mill. This is general result that tensile properties in sulfur cross-linked composites are higher than those in peroxide cross-linked composites. The observation in this study is in good agreement with general phenomenon.

Accordingly, the soft processing method is useful for the preparation of high performance lignin/rubber composites even at low content of filler (10 phr of lignin). Up to here, the mechanical behaviours of biocomposite prepared by the soft processing method were found to be different from the biocomposites prepared by conventional mixing method. This behaviour is probably due to the different of the morphological features. Thus, the samples were subjected to observe their morphologies and will be discussed in next section.

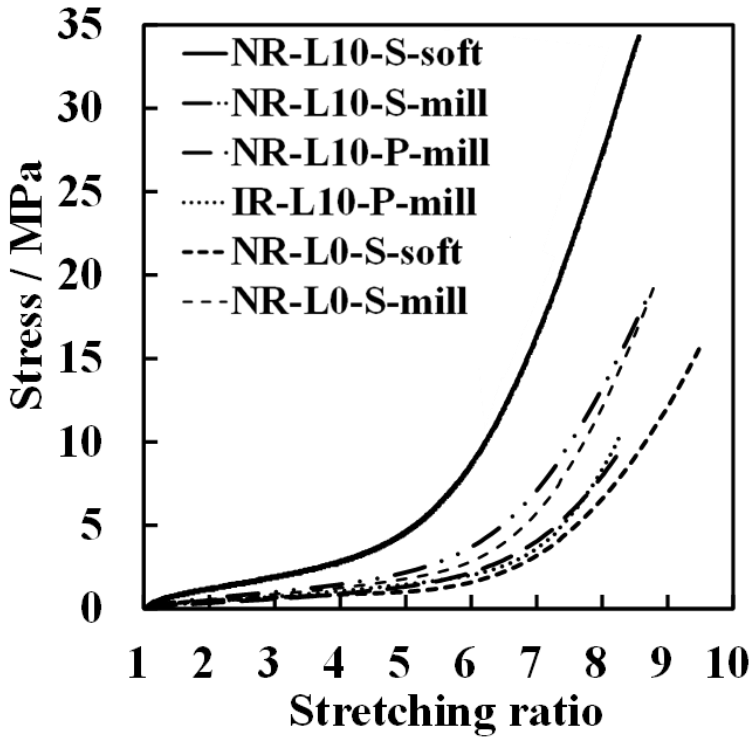

Figure 1.3 Tensile stress-strain curves of the composites and non-filled samples.

1.3.2 Morphology observations of lignin/NR biocomposite

Generally, lignin is autofluorescence material. Therefore, the laser scanning confocal microscopy (LSCM) was selected in order to elucidate morphologies of lignin in the rubber matrices of the composites. Figure 1.4 shows LSCM photographs of the composites, lignin powder, dry NR precipitated from the latex using 10% aqueous acetic acid solution, and the unfilled samples.

The observed LSCM image of NR-L10-S-soft was almost similar to that of NR-L0-S-soft. Both the dry NR latex and the solid NR show no fluorescence parts under the objective used in this study; therefore the fluorescence emissions from

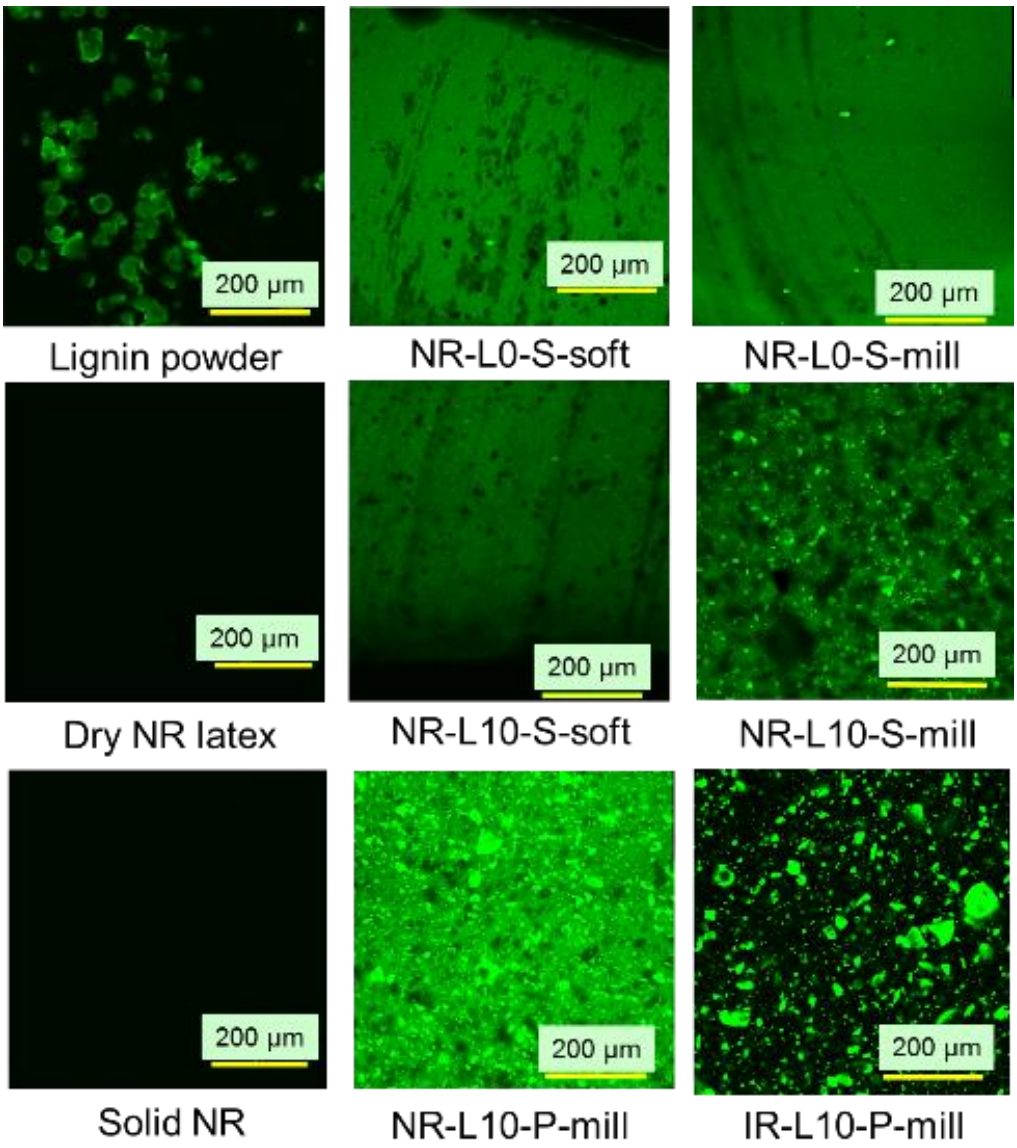

Figure 1.4 LSCM images of samples.

NR-L10-S-soft and NR-L0-S-soft were mainly ascribed to the sulfur cross-linking reagents. Thus, these results clearly suggest the presence of a fine dispersion of lignin in NR-L10-S-soft, i.e., a size of lignin is indicated to be less than 100 nm in the NR matrix of NR-L10-S-soft. In other words, the dispersed lignin was of the size smaller than the

wavelength of the light used in the detector (530 nm). It is to be noted that the LSCM image of NR-L0-S-soft exhibit only the fluorescence emission of cross-linking reagents. Besides, the fluorescence emission parts in NR-L10-S-soft correspond to both lignin and cross-linking reagents.

Meanwhile, the LSCM images of NR-L0-S-mill and NR-L10-S-mill are difference, i.e., the fluorescence emissions from NR-L0-S-mill were more homogeneous than those from NR-L10-S-mill. In the other word, LSCM image of NR-L10-S-mill exhibited some aggregates lignin whose size *ca.* 10 μm. In addition, the fluorescence emissions of NR-L10-P-mill and IR-L10-P-mill are almost similar to those of NR-L10-S-mill. It is worth noted that NR-L10-S-soft did not show any lignin powder particles of a similar size to those detected in the lignin milled samples.

TEM observation was then conducted for NR-L10-S-soft. Figure 1.5 shows a TEM photograph, where the two-phase structure in the lignin/NR biocomposite was clearly detected. Dark parts and bright parts represent the lignin and the rubber matrix, respectively. Similarly to the *in situ* silica filled NR nanocomposites in previous study by our research group [13,14], the lignin was clearly observed to be located around the rubber particles to form a network-like structure of lignin. Inside of rubber matrix, there was little lignin or almost no lignin.

Namely, the rubber particles in the NR latex provide templates for formation of the lignin network around the NR phases during drying the liquid mixture of lignin and NR in the film formation state. This is similar to the mechanism of the formation of *in situ* silica network in our previous studies [13,14,16]. In addition, the network of lignin is considered to partially consist of a continuous phase of the regenerated lignin from the solution. This supposed that the ionic sites in the sodium lignosulfonate may interact

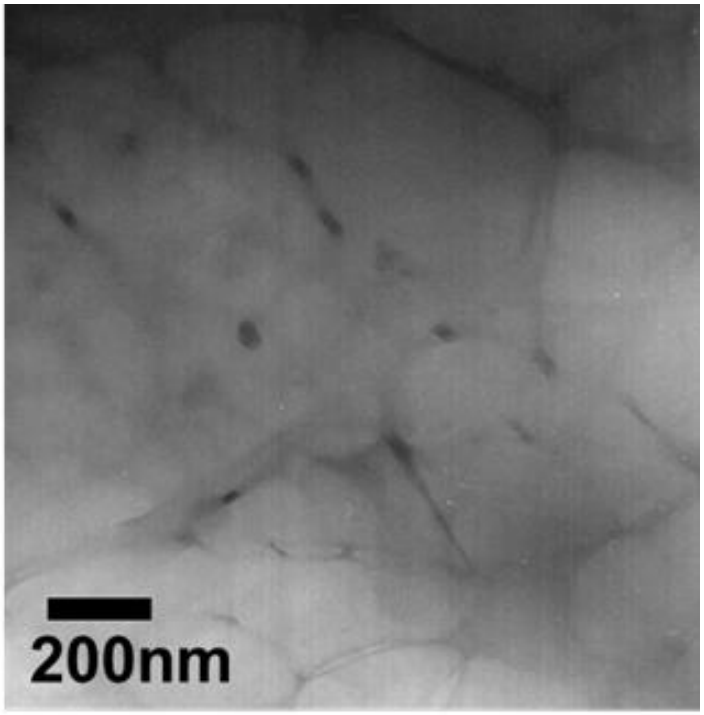

Figure 1.5 TEM photograph of NR-L10-S-soft.

with each other to aggregate like an ionomer after the drying.

The height and phase images of SPM in Figure 1.6 (a) and (b), respectively, confirm the morphological feature of NR-L10-S-soft. The light beige and brown colors show hard and soft phases, i.e., lignin and NR, respectively. This lignin morphology endows NR-L10-S-soft with the excellent tensile properties, as shown in Figure 1.3. Figure 1.6 (a) shows clearly network-like structure of lignin which was located around the rubber particles in the NR latex. According to the results of this study, they suggest that organic biofiller of lignin also supports the following idea for the reinforcement of rubber, when the soft processing method was utilized to prepare the nanocomposite: “Not the highest dispersion but to get a certain dispersion that may be favorable to form a network-like

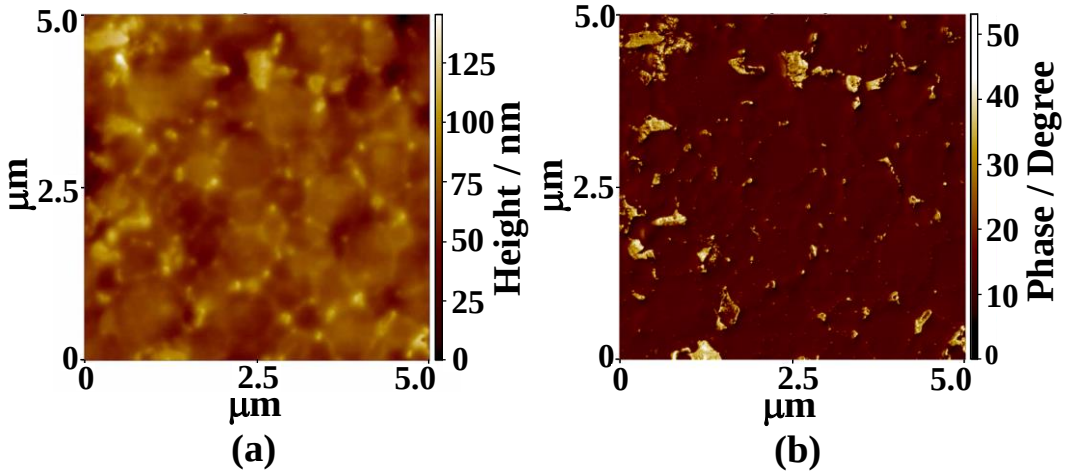

Figure 1.6 SPM images of NR-L10-S-soft. (a) a height image and (b) a phase image.

structure of nanofiller is to be the best dispersion in terms of rubber reinforcement." Up to now, "the better is the dispersion, the more is the reinforcement" has been the popular belief among rubber scientists and technologists. However, the observed reinforcement effect in this study clearly shows the role of nanofiller networks for the reinforcement of rubber similarly to the inorganic fillers [16-30]. Moreover, the effect of "bound rubber" must also be taken into account in the reinforcement of NR-L10-S-soft. Bound rubber is well known to be rubber that strongly interact with the filler by physical adsorption and chemisorption and/or cross-linking of rubber molecules on the filler surface [31-36], and it has been a central focus in rubber science and technology. It is clearly seen that bound rubber was detected in NR-L10-S-soft as can be seen in Figure 1.6 (b). Thus, this may be also one of factors to enhance mechanical properties in NR-L10-S-soft.

1.4 Conclusion

According to these results, the lignin soft biocomposite with high performance and eco-friendly was successfully prepared by using two sustainable natural resources, i.e., natural rubber (NR) latex and lignin. Typically, lignin is a waste from kraft process produced by paper-pulping industries, but it can be used as effective reinforcing filler for biomass NR when it is mixed with the NR latex *via* the soft processing method. The formation of the network-like agglomerates containing the bound rubber is essential for application of lignin as a high efficient filler for rubber as in the cases of conventional carbon black or particulate silica. On the other hand, the high performance biocomposite with network-like structure of lignin were successfully prepared. Thus, the results of this study are the first report to use lignin to prepare high performance biocomposite as far as the author known. This will be useful for the development of lignin-reinforced polymer composites for sustainable materials.

References

1. S. Kohjiya, *Natural rubber: From the odyssey of the Hevea tree to the age of transportation*, Smithers RAPRA, Shrewsbury, 2015.

2. Y. Hirata, H. Kondo, Y. Ozawa, *Chemistry, Manufacture and Applications of Natural Rubber*, eds S. Kohjiya, Y. Ikeda, Woodhead/Elsevier, Amsterdam, 2014, Chapter 12, 325-352.

3. J. J. Keilen, A. Pollak, *Ind. Eng. Chem.*,1947, **39**, 480.

4. J. J. Keilen, W. K. Dougherty, W. R. Cook, *Ind. Eng. Chem.*, 1952, **44**, 163.

5. T. R. Griffith, D. W. MacGregor, *Ind. Eng. Chem.*, 1953, **45**, 380.

6. F. J. Tibenham, N. S. Grace, *Ind. Eng. Chem.*, 1954, **46**, 824.

7. Anon, *Chem. Eng. News*, 1957, **35**, 28.

8. S. Yamashita, S. Kohjiya, *Wood processing and utilization*, eds J. F. Kennedy, G. O. Philips, P. A. Williams, Ellis Horwood, Chichester, 1989, Chapter 23.

9. V. K. Thakur, M. K. Thakur, P. Raghavan, M. R. Kessler, *ACS Sustainable Chem. Eng.*, 2014, **2**, 1072.

10. C. Jiang, H. He, H. Jiang, L. Ma, D. M. Jia, *eXPRESS Polymer Letters*, 2013, **7**, 480.

11. E. Ten, W. Vermerris, *J. Appl. Polym. Sci.*, 2015, **132**, 42069(1).

12. T. Phakkeeree, *Preparation, structure, and properties of natural rubber/lignin nanocomposites*, Master thesis of Mahidol University, 2009.

13. A. Tohsan, P. Phinyocheep, S. Kittipoom, W. Pattanasiriwisawa, Y. Ikeda, *Polym. Adv. Technol.*, 2012, **23**, 1335.

14. A. Tohsan, Y. Ikeda, *Chemistry, manufacture and applications of natural rubber*, eds S. Kohjiya, Y. Ikeda, Woodhead/Elsevier, Cambridge, 2014, Chapter 6, 168-192.

15. http://www.npchem.co.jp/english/product/lignin/

16. A. Tohsan, R. Kishi, Y. Ikeda, *Colloid Polym. Sci.*, 2015, **293**, 2083.

17. F. Bueche, *Reinforcement of elastomers*, ed G. Kraus**,** Interscience, New York, 1965, Chapter 1, p.1.

18. J. B. Donnet, R. C. Bansal, M.-J. Wang, *Carbon Black*, Marcel Dekker, New York, 1993.

19. G. Heinrich, M. Klüppel, *Adv. Polym. Sci*., 2002, **160**, 1.

20. M. Klüppel, *Adv. Polym. Sci*., 2003, **164**, 1.

21. S. Kohjiya, A. Katoh, J. Shimanuki, T. Hasegawa, Y. Ikeda, *J. Mater. Sci.*, 2005, **40**, 2553.

22. S. Kohjiya, A. Kato, T. Suda, J. Shimanuki, Y. Ikeda, *Polymer*, 2006, **47**, 3298.

23. A. Kato. J. Shimanuki, S. Kohjiya, Y. Ikeda, *Rubber Chem. Technol.*, 2006, **79**, 653.

24. S. Kohjiya, A. Kato, Y. Ikeda, *Prog. Polym. Sci.*, 2008, **33**, 979.

25. F. Deng, M. Ito, T. Noguchi, Y. A. Kim, M. Endo, Q.-S. Zheng, *ACS Nano*, 2011, **5**, 3858.

26. A. Kato, Y. Ikeda, S. Kohjiya, *Polymer Composites*, Vol. 1, eds S. Thomas, K. Joseph, S. K. Malhotra, K. Goda, M. S. Sreekala, Wiley-VCH Verlag GmbH & Co., Weinheim, 2012, Chapter 17, 515-543.

27. A. Kato, Y. Ikeda, R. Tsushi, Y. Kokubo, N. Kojima, *Colloid Polym. Sci.*, 2013, **291**, 2101.

28. A. Kato, Y. Kokubo, R. Tsushi, and Y. Ikeda, *Chemistry, manufacture and applications of natural rubber*, eds S. Kohjiya, Y. Ikeda, Woodhead/Elsevier, Cambridge, 2014, Chapter 7, 193-215.

29. Y. Ikeda, A. Tohsan, *Colloid Polym. Sci*., 2014, **292**, 567.

30. A. Kato, A. Tohsan, S. Kohjiya, T. Phakkeeree, P. Phinyocheep, Y. Ikeda, *Progress in rubber nanocomposites*, eds S. Thomas, H. J. Maria, Woodhead/Elsevier, United Kingdom, 2016, Chapter 12, pp. 415-461.

31. P. B. Stickney, R. D. Falb, *Rubber Chem. Technol.*, 1964, **37**, 1299.

32. G. Kraus, *Reinforcement of elastomer*, Interscience, New York, 1965.

33. G. Kraus, *Rubber Chem. Technol.*, 1965, **38**, 1070.

34. A. K. Sircar, A. Voet, *Rubber Chem. Technol.*, 1970, **43**, 973.

35. S. Fujiwara, K. Fujimoto, *Rubber Chem. Technol.*, 1971, **44**, 1273.

36. G. Kraus, *Science and Technology of Rubber*, ed F. R. Eirich, Academic Press, New York, 1978, Chapter 8, 339-364.

CHAPTER 2

CHAPTER 2

Effect of Lignin Content on Mechanical Properties of Lignin/Natural Rubber Soft Biocomposites

2.1 Introduction

The rising consciousness of environment, depletion of petroleum resources, and health concerns are interested nowadays. Hence, the development of sustainable materials derived from biorenewable resources has been focused. Natural rubber (NR) is an essential sustainable soft material. It is the only agricultural product among rubbers, and only one polymeric hydrocarbon produced in the biological world [1]. Therefore, NR can be continuously produced even after the depletion of fossil fuels (petroleum and coal). NR is well known to exhibit various outstanding properties on the basis of highly elastic property due to entropy [2-4]. The characteristic of NR cannot be easily mimicked by synthetic rubbers, even though the polymer science and technology have been significantly developed in last century.

NR based soft composites have been regarded as one of the most successful materials for industrial products among many polymer composites. In terms of sustainable development and carbon neutral products, biofillers such as cellulose nanofibers, biosilica, and lignin have been attracted by many researchers. Among them, lignin is the second most abundant biopolymer next to cellulose, and it is being focused on the effective use of lignin waste from kraft processes [5,6]. Typically, lignin from kraft process is used as a low value fuel in the paper-pulping manufacturing and is highly hydrophobic and contains aliphatic thiol groups [7-9].

Is it truly difficult for lignin to play a role to reinforce rubbers? To answer this question, a trial to use a soft processing method was conducted and the preliminary positive results were reported in previous chapter [19]. In our research group, the soft processing method taking an advantage of NR latex has been focused in order to prepare the novel high performance NR composites [20]. The method is based on our concept that a filler network is formed in a NR matrix by using NR particles in the NR latex as templates. The quite useful reinforcement effect of the filler network for NR has been recognized: For example, the role of filler network on high performance of *in situ* silica/NR nanocomposites was clearly shown by using this technique [21,22]. Recently, lignin was also successfully used as effective reinforcing filler for NR similarly to the inorganic fillers, in which 10 parts per one hundred rubber by weight (phr) of lignin was mixed with NR using this soft processing method [19]. This method is very simple and seems to be easily utilized to the practical application for rubber productions. However, the characteristics of only 10 phr lignin-filled NR nanocomposite were briefly reported in the previous chapter [19]. Thus, the effect of lignin contents on the tensile properties of lignin filled NR composites with their unique morphological features is investigated in this chapter. The results will be very useful to reveal the role of organic filler "lignin" for the reinforcement of NR.

2.2 Experimental

2.2.1 Materials

The biocomposites composed of lignin and NR were prepared by the soft processing method similar to the preparation method in Chapter 1: high ammonia NR latex of 100 ml was mixed with sulfur cross-linking reagents, and followed by mixing with each

alkali aqueous solution of 5, 10, 20 or 40 phr of sodium lignosulfonate, respectively. The films were prepared by similarly preparation method to the previous chapter. The biocomposites having lignin of 5, 10, 20 and 40 phrs are abbreviated as NR-L5-S-soft, NR-L10-S-soft, NR-L20-S-soft and NR-L40-S-soft, respectively. In addition, an unfilled sample (NR-L0-S-soft) was also prepared by the soft processing method as a reference. In the sample codes, “L”, “number”, “S” and “soft” mean lignin, a content of lignin in phr, a sulfur cross-linking, and the soft processing, respectively.

As reference samples, lignin filled NR biocomposites were prepared similar to the preparation method for sulfur cross-linking in Chapter 1. Each rubber compound was molded into a sheet of 1 mm thickness by heat pressing at 140 ^{o}C for 12 min, which was the optimal cure time determined by the cure measurement at 140 ^{o}C by JSR Curelastometer III. The biocomposites having lignin of 5, 10, 20 and 40 phr are abbreviated as NR-L5-S-mill, NR-L10-S-mill, NR-L20-S-mill and NR-L40-S-mill, respectively. An unfilled lignin NR sample (NR-L0-S-mill) was also prepared by using the same recipe. In the sample codes, “L”, “number”, “S” and “mill” mean lignin, a content of lignin in phr, a sulfur cross-linking, and conventional mixing method, respectively.

2.2.2 Raman spectroscopy

NR-L10-S-soft and NR-L40-S-soft were directly subjected to Raman spectroscopy without any treatments by Nicolet iS50 FT-IR with the Raman module (Thermo Fisher Scientific Inc.) using diode laser at 1064 nm. The resolution and accumulation time were 8 cm^{-1} and 500 times, respectively. Raman spectral bands of NR-L0-S-soft, NR-L10-S-soft and NR-L40-S-soft are shown in Figure 2.1. The bands indicating

hydrocarbon chains of *cis*-1,4-polyisoprenes of NR, were assigned at ν = 1666 cm^{-1} (C=C stretching), 1288 cm^{-1} (CH bending), 1375 cm^{-1} (CH_3 asymmetric deformation), 1451 and 1362 cm^{-1} (CH_2 deformation), and 1315 cm^{-1} (CH_2 twisting). In addition, a Raman spectral bands which are contributed to lignin was found at ν = 1600 cm^{-1} (C-C of aromatic ring symmetric stretching), 1635 cm^{-1} (probably ascribable to C=C stretching of coniferaldehyde/sinapaldehyde) and 1410 cm^{-1} (phenolic OH bending/ CH_3 bending) [23].

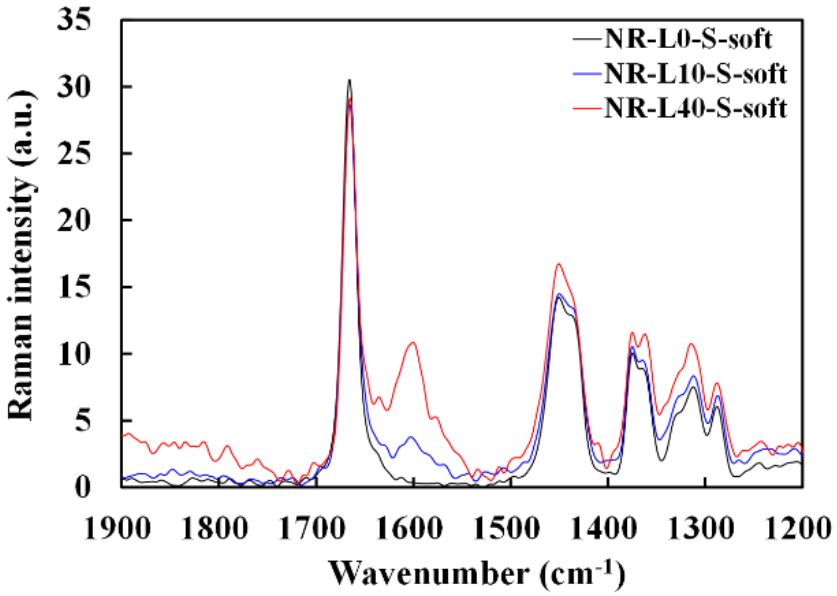

Figure 2.1 Raman spectra of NR-L0-S-soft, NR-L10-S-soft and NR-L40-S-soft.

2.2.3 Tensile measurements

Tensile properties were measured at r.t. using the same machine and conditions of measurements as described in Chapter 1 section 1.2.3 that a stretching speed of 100 mm/min, i.e., the strain speed was about 4.98 per min. A stretching ratio (α) is defined as "$\alpha = l/l_0$", where l is a length after deformation, and l_0 is an initial length,

respectively.

2.2.4 Measurement of network-chain density

A network-chain density (ν) of the films of lignin filled NR biocomposites was evaluated on the basis of the classical theory of rubber elasticity as follows; [24]

$$\sigma = \nu RT(\alpha - \frac{1}{\alpha^2}) \quad (1)$$

where σ is tensile stress, R is gas constant, α is stretching ratio and T is absolute temperature.

2.2.5 Morphology observations by laser scanning confocal microscopy and scanning probe microscopy

Laser scanning confocal microscopy (LSCM) was performed using the same machine, wavelength and detector which were described in Chapter 1 section 1.2.4. In addition, three-dimensional images were also obtained with a 100× objective (CFI Plan Apochromat 100×/1.4 DIC VC, Nikon Co., Japan) using NIS-Elements software, Nikon Co., Japan.

Scanning probe microscopy (SPM) observation was also performed using the same machine, probes and preparation of surface for sample as described in Chapter 1 section 1.2.4.

2.2.6 Evaluation of Payne effect

Payne effect was investigated at *ca.* 25 °C by using a rheometer MR-500 (Rheology

Co., Japan) at 1 Hz of frequency and rotation angles between 0.01 and 15°. The size of the specimen was 8 × 8 × thickness in mm^3.

2.2.7 Dynamic mechanical analysis

Dynamic mechanical properties were evaluated using a Rheospectolar DVE-4 instrument in a tension mode at a frequency of 10 Hz and temperature range from -130 °C to 150 °C at a heating rate of 2 °C/min. The size of the specimen was 25 × 5 × thickness in mm^3. The applied static force was automatically controlled, and the dynamic strain was ± 3 μm. Storage modulus (E′) and loss factor (tan δ) were measured as a function of temperature. The tensile mode was used, and the applied static force was automatically controlled.

2.3 Results and discussion

2.3.1 Tensile properties of lignin filled NR biocomposites

Tensile stress-strain curves of NR biocomposites containing 5, 10, 20 and 40 phr of lignin, which were prepared by the soft processing and conventional mixing methods, are illustrated in Figure 2.2 against those of unfilled samples. By repeating a few times measurements, the good reproducibility of tensile properties for all samples was obtained with the unbiased sample standard deviation (σ) < 0.382 for the stresses at the stretching ratios of 3.0, 5.0 and 7.0. Only the tensile strength (T_B) and stretching ratio at break (E_B) possessed σ < 4.16. In addition, the fracture properties have been well-known to have effects of cuts and/or scratches on the surfaces of specimens. Thus, the tensile properties using the samples with the highest T_B and E_B in Figure 2.2 are summarized with their network-chain densities in Table 2.1. A reinforcement effect of

the lignin to increase the stresses at low stretching ratios was detected in both series. Specifically, the tensile stresses of the lignin-filled NR biocomposites prepared by the soft processing method were found to significantly increase with increasing the lignin content, similar to conventional carbon black (CB) filled systems. For example, the tensile stresses of NR-L5-S-soft at α = 3.0, 5.0 and 7.0 were about 160%, 330% and 450% higher than those of an unfilled sample (NR-L0-S-soft), respectively. Note that the improvement of the tensile strength and stretching ratio at break was difficult for the lignin/NR soft biocomposites, although the soft processing is useful for the utilization of sodium lignosulfonate as a reinforcing filler for rubber. This point is our challenge in near future. On the other hand, the increment in the tensile stresses of NR-L5-S-mill was 0%, 6% and 7% at α = 3.0, 5.0 and 7.0, respectively, when compared to unfilled NR (NR-L0-S-mill). Unlike nano-sized fillers, the direct incorporation of micron-sized lignin to the rubber matrices by conventional milling was not efficient to bring about the high performance properties even when sodium lignosulfonate with ionic sites was used. However, the soft processing is useful for the utilization of sodium lignosulfonate as reinforcing filler for rubber.

In the lignin filled NR biocomposites prepared by this soft processing (hereafter, it is called as “Lignin/NR soft biocomposites” in this study), the different features of tensile properties seem to be distinguishable into two groups on the basis of the stress-strain curves. At first, NR-L5-S-soft and NR-L10-S-soft, which provided the considerably high up-turn stresses at their large strains and their stress-strain curves, were very similar. In addition, the tensile strengths at break of these biocomposites were surprisingly larger than that of NR-L0-S-soft. In the second, NR-L20-S-soft and NR-L40-S-soft did not show much abrupt up-turn stresses at a high strain like

NR-L5-S-soft and NR-L10-S-soft, although their stresses significantly increased from the low stretching ratios. These results suggest that the reinforcement mechanism resulting from filling lignin was different for the two groups, although the processing was same among the biocomposites.

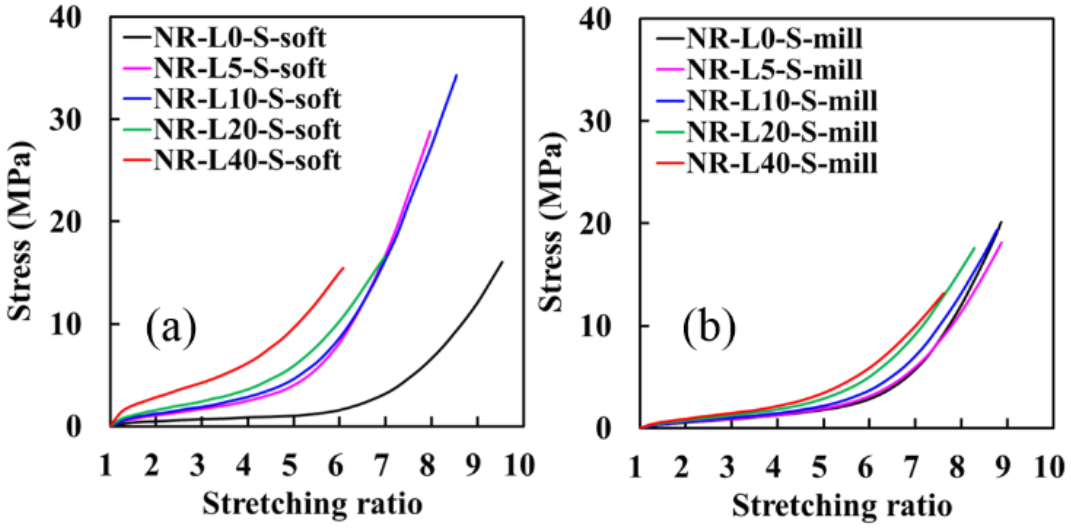

Figure 2.2 Tensile stress-strain curves of the lignin filled NR biocomposites with those of unfilled samples. The soft processing method (a) and the conventional mixing methods (b).

In general, the abrupt upturn of stress at high strains for cross-linked NR is ascribable to the strain-induced crystallization (SIC) behaviour. It is also well known that significant increases of tensile stresses at low strains are due to the filler-filler interaction in the composites. Therefore, the characteristics of the first group are predicted to relate to the acceleration of SIC by filling the lignin using the soft processing method. The second may be mainly concerned with a dispersion of the lignin in the rubber matrix. In order

Table 2.1 Properties of lignin filled NR biocomposites prepared by soft processing and conventional methods at different lignin contents

Sample code	Lignin content (phr)[a]	Network-chain density[b] $\times 10^4$ (mol cm^{-3})	Stress at $\alpha = 3$ (MPa)	Stress at $\alpha = 5$ (MPa)	Stress at $\alpha = 7$ (MPa)	T_B[c] (MPa)	E_B[d]
NR-L0-S-soft	0	1.4	0.7	1.0	3.2	13.9	9.5
NR-L0-S-mill	0	1.2	0.9	1.8	5.7	18.8	8.9
NR-L5-S-soft	5	2.4	1.8	4.3	17.7	27.2	7.8
NR-L5-S-mill	5	1.2	0.9	1.9	6.0	17.1	8.8
NR-L10-S-soft	10	2.6	1.9	4.7	17.0	24.6	7.8
NR-L10-S-mill	10	1.5	1.0	2.1	7.1	19.2	8.8
NR-L20-S-soft	20	3.2	2.4	6.0	-	15.1	6.8
NR-L20-S-mill	20	1.7	1.2	2.7	8.4	17.4	8.3
NR-L40-S-soft	40	7.9	4.2	9.6	-	12.2	5.5
NR-L40-S-mill	40	2.5	1.4	3.2	9.4	11.8	7.5

[a] Parts per one hundred rubber by weight.

[b] Estimated on the basis of the classical theory of rubber elasticity using eqn. (1).

[c] Tensile strength at break.

[d] Stretching ratio at break.

to confirm these points, several characterizations were carried out for the biocomposites in this study. As already discussed in Chapter 1[19], the soft processing was found to form the specific morphology of lignin like a filler network around the rubber phases. Thus, the morphological features of the biocomposites were compared and discussed

next in order to reveal the difference of the reinforcement effects between the two groups. In this paper, the Lignin/NR soft biocomposites with 10 and 40 phr lignins are focused as typical samples for each group.

2.3.2 Morphological characteristics of lignin/NR soft biocomposites

Morphologies of lignin in the rubber matrices of the biocomposites were investigated by using laser scanning confocal microscopy (LSCM). Figure 2.3 illustrates the LSCM photographs of the biocomposites, lignin powder, solid NR, dry NR precipitated from the latex using 10% aqueous acetic acid solution, and the unfilled samples. Notably, any special treatment for the samples was not required due to an autofluorescence of lignin for the observations. The diameter of lignin powder was detected to be *ca.* 20 – 45 μm. The gum solid NR and the dry NR from the latex did not show any autofluorescence under the objective used in this LSCM images. Therefore, the fluorescence phenomena from the unfilled samples, i.e., NR-L0-S-soft and NR-L0-S-mill were mainly ascribed to the sulfur cross-linking reagents. The observed LSCM image of NR-L10-S-soft was almost same with that of NR-L0-S-soft even though the former contained the lignin. Furthermore, the LSCM image of NR-L40-S-soft was different with those of NR-L10-S-soft and NR-L0-S-soft, where the black parts were not clearly detected but a homogeneous green phase was much obviously seen instead. This difference suggest two possible phenomena: The lignin may be finely dispersed in the NR matrix and the lignin may play a role to well disperse the sulfur cross-linking reagents in the matrix. The considerations were apparently supported by comparing with LSCM images of NR-L10-S-mill and NR-L40-S-mill. As shown in Figure 2.3, their images showed the fluorescence emission from both the

sulfur cross-linking reagents and the lignin particles as a green background and brighter green dots, respectively. The diameter of lignin powder was found to become small by milling, and it was *ca.* 5 – 9 μm in NR-L40-S-mill. In addition, bigger black parts were detected in NR-L10-S-mill than NR-L10-S-soft and NR-L0-S-soft. It is worth noted that NR-L10-S-soft and NR-L40-S-soft did not show any lignin powder particles of a similar size to those detected in the lignin milled samples. These results clearly suggest the presence of better dispersion of lignin in the biocomposites prepared by the soft processing method than in the biocomposites prepared by the conventional mixing method. In addition, the size of lignin in Lignin/NR soft biocomposites was indicated to be less than 100 nm by judging the resolution of LSCM in this study.

The three-dimensional LSCM images of NR-L40-S-soft and NR-L40-S-mill more clearly supported this consideration as shown in Figure 2.4, where the lengths were *ca.*120 μm, and the thickness was *ca.*40 μm, respectively. The fluorescence emissions from NR-L40-S-soft and NR-L10-S-soft may be mainly attributed to the sulfur cross-linking reagents, because the dry NR from the latex did not show any fluorescence under the objective used in this experimental condition. The question then is what the difference between the morphology of NR-L10-S-soft and NR-L40-S-soft is. In order to reveal the characteristic features, a scanning probe microscopy (SPM) was conducted for NR-L10-S-soft and NR-L40-S-soft in the next.

Phase and height SPM images of NR-L10-S-soft and NR-L40-S-soft are shown in Figure 2.5 with those of NR-L0-S-soft. In their phase images, bright and dark parts correspond to hard and soft phases, indicating the lignin and the NR phases in NR-L10-S-soft and NR-L40-S-soft, respectively. As expected similarly to the *in situ* silica filled NR nanocomposites prepared by the soft processing [21,22,25,26], the lignin

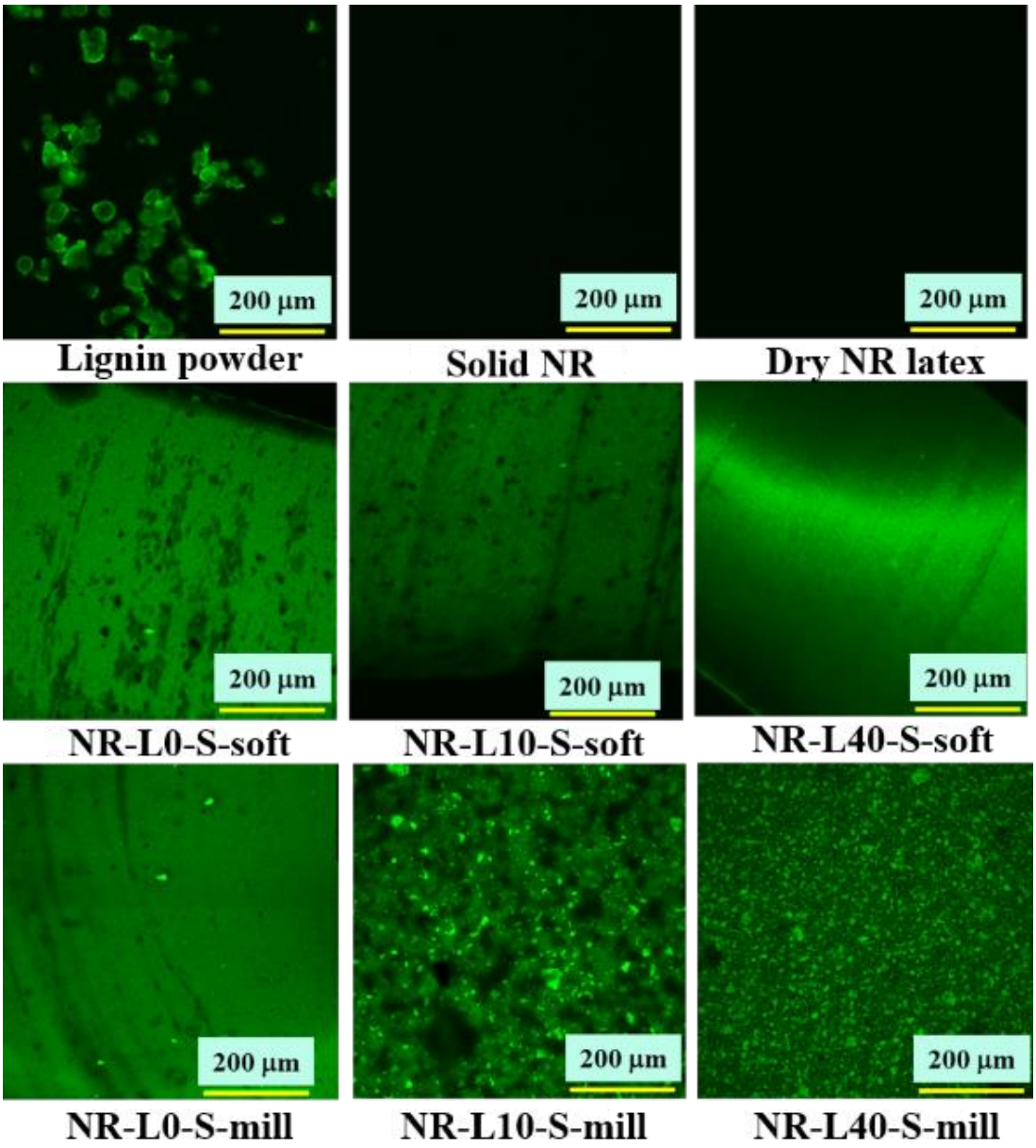

Figure 2.3 LSCM images of the lignin filled NR biocomposites, lignin powder, solid NR, dry NR precipitated from the latex using 10% aqueous acetic acid solution, and the unfilled samples.

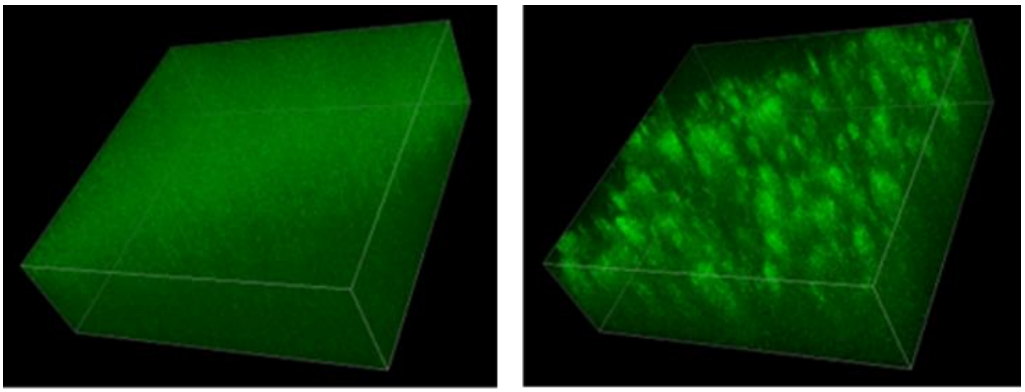

Figure 2.4 Three-dimensional LSCM images of NR-L40-S-soft and NR-L40-S-mill, where the lengths and the thickness were *ca.*120 μm and *ca.* 40 μm, respectively.

seemed to be located around the NR particles in the latex during film forming, , to result in the selective formation of lignin phases around the rubber phases [19]. Namely, network-like structures of lignin in the biphasic structured morphologies were detected inboth NR-L10-S-soft and NR-L40-S-soft. The height images also clearly showed the filler network-like structures. Note that the lignin phases became large by the increase of lignin. The shape of NR particles in the latex was well reflected to the soft NR phases. Especially, an arc shaped interfaces between the lignin and rubber were clearly recognized in NR-L40-S-soft as shown in Figure 2.5.

It is worth noting that the size of rubber phases of NR-L10-S-soft and NR-L40-S-soft were very similar to that of beige colored region of NR-L0-S-soft shown in Figure 2.5, which also supported the aggregation of lignin components around the rubber particles in the NR latex. The mechanism of the formation of lignin aggregates like a network may be similar to that of *in situ* silica network using NR latexes reported in our previous works

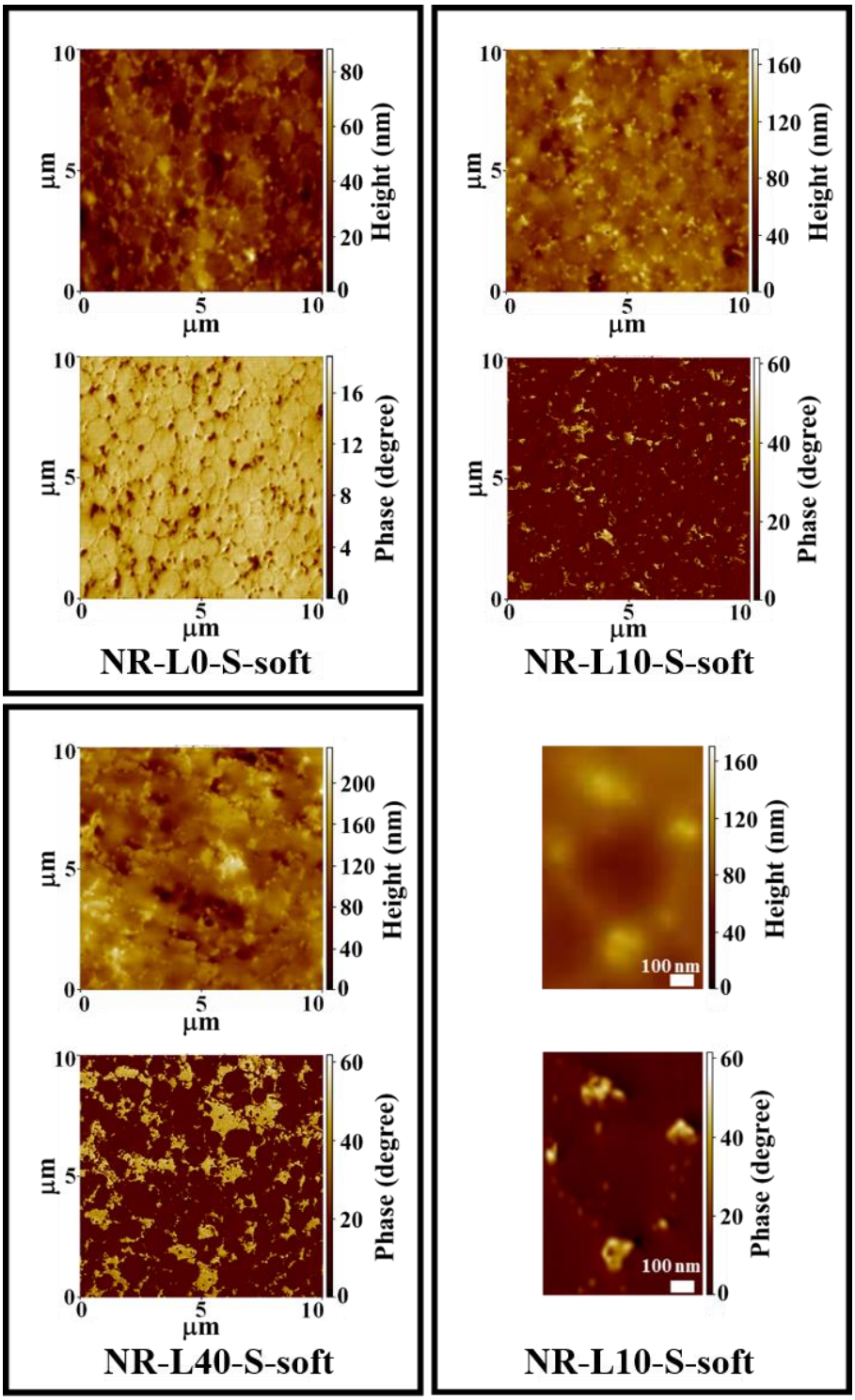

Figure 2.5 SPM height and phase images of NR-L0-S-soft, NR-L10-S-soft, NR-L40-S-soft and the magnified height and phase images of NR-L10-S-soft.

[22,25,26], because the lignin used in this study possesses ionic sites of sodium sulfonate. In the NR latex, the ionic sites in the lignin may have interacted with the non-rubber components of the surface of NR particles *via* Coulomb interaction. In fact, the lignin around the NR phases was observed to be well wetted by NR, resulting in the unclear lignin/rubber interface as shown in Figure 2.5. The SPM results on NR-L40-S-soft much clearly suggest that the organic biofiller of lignin supported the following idea for the reinforcement of rubber than those of NR-L10-S-soft, when the soft processing method was utilized to prepare the nanocomposite: "Not the highest dispersion but to get a certain dispersion that may be favorable to form a network-like structure of nanofiller is to be the best dispersion in terms of rubber reinforcement" [19,20]. This unique morphology endowed the lignin-filled NR biocomposites prepared by the soft process with the excellent tensile properties as shown in Figure 2.2. The network-like structure of lignin in the NR composites was confirmed by results of the Payne effect as discussed in the following section.

When the morphologies between Lignin/NR soft biocomposites and NR-L0-S-soft are compared, a following unique point is appeared: The hardness of the interface phase between the rubber phases (the beige phases) changed after the filling of lignin. In the unfilled sample, the interface was softer than the rubber phases, however, the lignin made it harder than the rubber phases. This phenomenon clearly shows that the lignin plays a role to reinforce the interface. Because sodium lignosulfonate is an organic material containing the ionic sites, the compatibility of lignin with the non-rubber components on the NR particles in the NR latex becomes good to result in the hard interfaces between the rubber phases after drying. In Figure 2.5, it is also noted that the NR phases were spherical and/or ellipse shaped ones, its size distribution was relatively

homogeneous and its average diameter was *ca.* 1 μm. Even after the filling of lignin, the size of NR phases was not much changed.

Generally, the rubber particles in the NR latex coalesce to form a relatively strong film during drying, where the surface boundaries of the coalesced rubber particles are formed. The main components of the boundaries were reported to be non-rubber components such as phospholipids, fatty acids and so on. [27-29] Therefore, the soft phases, i.e. the dark brown colored parts, which were dispersed around the NR phases of NR-L0-S-soft in Figure 2.5, are supposed to be non-rubber components even after the sulfur cross-linking under the reaction condition of this study. Therefore, our SPM results clearly suggest that the interface ascribed to the non-rubber components was much softer than the matrix of sulfur cross-linked NR. The surfactants used for dispersing cross-linking reagents in the vulcanization may have more or less influenced the softness of the interface.

2.3.3 Mechanical properties of lignin/NR soft biocomposites

Typically, a difference of shear storage modulus (G′) at small and large deformations reflects a filler-filler interaction in the filler-filled rubber materials, known as "Payne effect". In order to evaluate the degree of filler-filler interaction of Lignin/NR soft biocomposites, variations of G′ over 10^{-2} to 10^{3} % strain at 1 Hz of frequency for the composites with 10 and 40 phr lignin contents were investigated, and results are shown in Figure 2.6. It is worth noted that significantly different tendencies were observed among the samples: The Payne effect of NR-L40-S-soft was much larger than that of NR-L10-S-soft and NR-L0-S-soft, which agreed well with those observed for the conventional carbon black or silica-filled rubber composites. The significant Payne

effect of NR-L40-S-soft suggests the presence of a stiff network-like structure of lignin with a high filler-filler interaction in the NR matrix. Even by the addition of small amount of lignin by the soft processing method, the Payne effect was clearly observed as shown in NR-L10-S-soft. The interface between the NR phases composed of the non-rubber components is supposed to be strengthened by filling of the lignin. With further increasing strain, no obvious change of the G′ for Lignin/NR soft biocomposites was found, leading to platform under the strain of 10 to 10^2 %. This indicated that the filler-filler interaction of the NR biocomposites would be destroyed almost completely even in a case of NR-L40-S-soft.

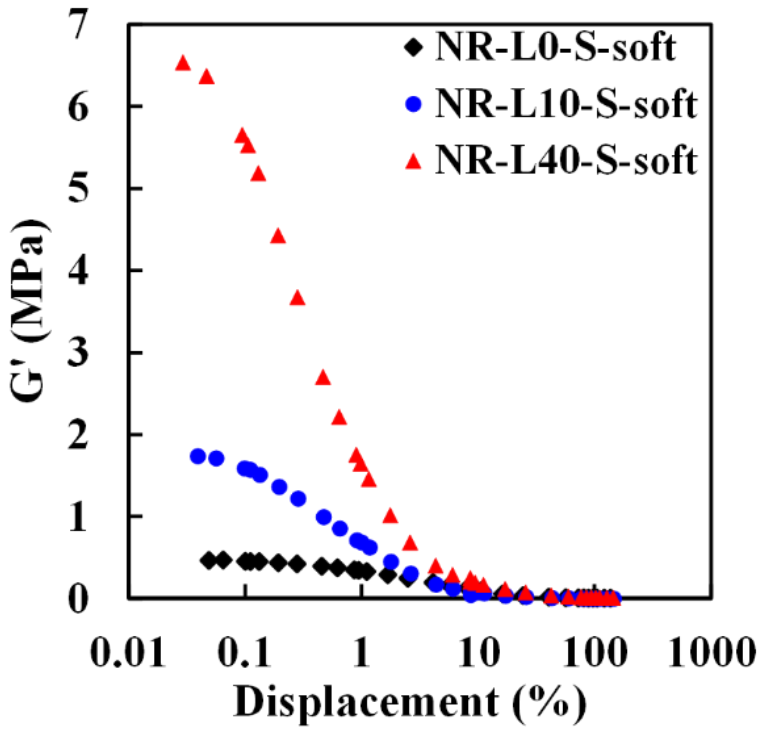

Figure 2.6 Payne effect of Lignin/NR soft biocomposites.

Figure 2.7 presents the temperature dependence of storage modulus (E′) and loss factor curve (tan δ) of Lignin/NR soft biocomposites with the unfilled sample prepared by the soft processing method. The E′ at 25 °C of Lignin/NR soft biocomposites was obviously enhanced by mixing the lignin contents, especially by filling of 40 phr lignin. The tendency of increase of E′ at 100 °C was similar to that of E′ at 25 °C. These results also suggest that the NR was effectively reinforced by the lignin when the soft processing method was used for preparing the rubber composites. Moreover, a reduction of loss factor (shown as a decrease of height of tan δ) was detected with increasing the lignin content in the NR biocomposites prepared by the soft processing method, indicating the higher restriction of movements for the rubber chains at the interface of the biphasic

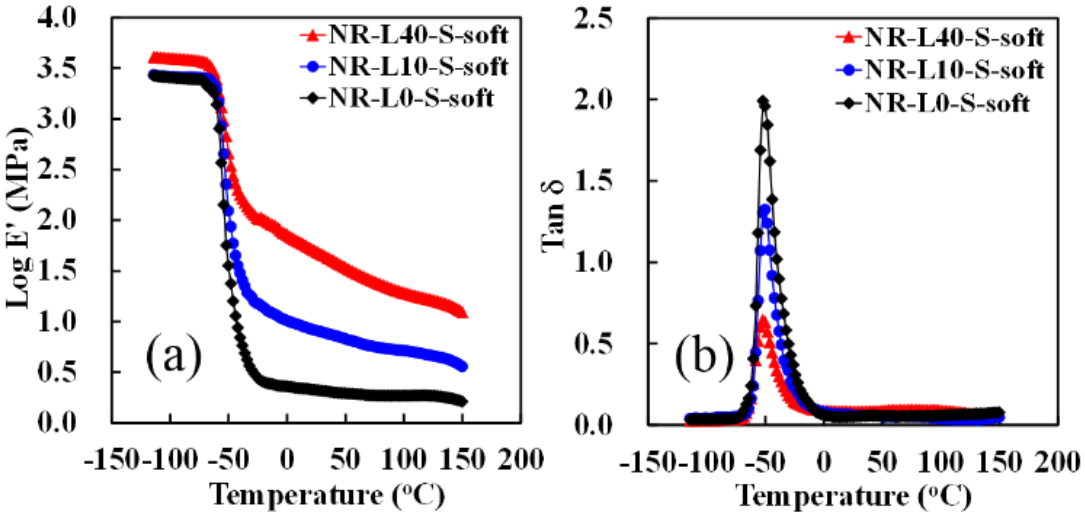

Figure 2.7 Temperature dependence of (a) E' and (b) tan δ for Lignin/NR soft biocomposites.

structures due to the higher lignin content. Therefore, it is suggested that Lignin/NR soft

biocomposites gave us not only the high modulus, but also high rigidity and stiffness, probably ascribed to the high filler-rubber interaction at the interface in Lignin/NR biocomposites. It is also worth noted, on the other hand, that Lignin/NR soft biocomposites shows a similar identical temperature of tan δ peak at -51 ^{o}C, referring to their glass transition temperatures (T_g), with that of NR-L0-S-soft as revealed in Figure 2.7. Because the lignin was located around the NR phases and the size of NR phases was similar among the samples, the T_g may be governed by the highly pure rubber phase in the core of rubber phases, not depending on the lignin contents in the samples prepared by the soft processing method.

2.4 Conclusion

The NR biocomposites with sodium lignosulfonates of 5, 10, 20 and 40 phr were successfully prepared by using the soft processing method. By this processing, the rubber particles in the NR latex acted as the templates for the formation of locally dispersed lignin around the rubber phases even at the high lignin filling. The significant Payne effect of 40 phr lignin filled NR biocomposite suggests the presence of a stiff network-like structure of lignin with a high filler-filler interaction in the NR matrix. Even by the addition of 10 phr lignin, the Payne effect was clearly observed, where the interface between the NR phases composing the non-rubber components is supposed to be strengthened by filling of the lignin. Based on the difference of their unique morphologies, the 40 phr lignin filled biocomposite provided the more excellent mechanical properties such as substantially higher tensile stresses, larger storage moduli and lower dissipative loss than the 10 phr lignin filled biocomposite. However, the low glass transition temperatures due to the pure rubber phases were observed in both

biocomposites. This is also the characteristic of the lignin filled NR biocomposites prepared by the soft processing method.

References

1. S. Kohjiya, *Natural rubber: From the odyssey of the Hevea tree to the age of transportation*, Smithers RAPRA, Shrewsbury, 2015.

2. A. D. Roberts, *Natural Rubber Science and Technology*, Oxford University Press, Oxford, 1988.

3. L. Mullins, *The Chemistry and Physics of Rubber-Like Substances*, ed. L. Bateman, MacLaren & Sons, London, 1963, Chapter 11, 301-328.

4. E. H. Andrews, A. N. Gent, *The Chemistry and Physics of Rubber-Like Substances*, ed. L. Bateman, MacLaren & Sons, London, 1963, Chapter 9, 225-248.

5. V. K. Thakur, M. K. Thakur, P. Raghavan, M. R. Kessler, *ACS Sustainable Chem. Eng.*, 2014, **2**, 1072.

6. E. Ten, W. Vermerris, *J. Appl. Polym. Sci.*, 2015, **132**, 42069(1).

7. P. J. M. Carrott Suhas, R. Carrott M. M. L., *Bioresource Technol.*, 2007, **98**, 2301.

8. W. Doherty, P. Mousavioun, C. Fellows, *Ind. Crops Products*, 2011, **33**, 259.

9. P. Wunning, *Biopolymers*, Wiley-VCH, Weinheim, 2004.

10. R. J. A. Gosselink, A. Abächerli, H. Semke, R. Malherbe, P. Käuper, A. Nadif, J. E. G. van Dam, *Ind. Crops Products*, 2004, **19**, 271.

11. M. A. De Paoli, L. T. Furlan, *Polym. Degrad. Stab.***,** 1985, **11**, 327.

12. C. G. Boeriu, D. Bravo, R. J. A. Gosselink, J. E. G. van Dam, *Ind. Crops Products*, 2004, **20**, 205.

13. C. Pouteau, P. Dole, B. Cathala, L. Averous, N. Boquillon, *Polym. Degrad. Stab.*, 2003, **81**, 9.

14. L. R. C. Barclay, F. Xi, J. Q. J. Norris, *Wood Chem.Tech.*, 1997, **17**, 73.

15. J. H. Lora, W. G. Glasser, *J. Polym. Environ.*, 2002, **10**, 39.

16. W. G. Glasser, S. Sarkanen, *Lignin: Properties and materials*, American Chemical Society, Washington, DC, 1989.

17. T. M. Garver, S. Sarkanen, *Renewable-resource materials: New polymer sources*, ed. C. E. Carraher Jr., L. H. Sperling, Plenum Press, New York, 1986, 287-304.

18. C. Jiang, H. He, X. Yao, P. Yu, L. Zhou, D. Jia, *J. Appl. Polym. Sci.*, 2015, **132**, 42044(1).

19. T. Phakkeeree, Y. Ikeda, H. Yokohama, P. Phinyocheep, R. Kitano, A. Kato, *J. Fiber Sci. Technol.*, 2016, **72,** 160.

20. A. Kato, A. Tohsan, S. Kohjiya, T. Phakkeeree, P. Phinyocheep, Y. Ikeda, *Progress in Rubber Nanocomposites*, eds. S. Thomas, H. J. Maria, Woodhead/Elsevier, United Kingdom, 2016, Chapter 12, 415-461.

21. Y. Ikeda, A. Tohsan, *Colloid Polym. Sci.*, 2014, **292**, 567.

22. A. Tohsan, R. Kishi, Y. Ikeda, *Colloid Polym. Sci.*, 2015, **293**, 2083.

23. L. R. G. Treloar, *The physics of rubber elasticity*; Clarendon Press, Oxford, 1975.

24. U. P. Agarwal, J. D. McSweeny, A. S. Ralph, *J. Wood Chem. Technol.*, 2011, **31**, 324.

25. A. Tohsan, P. Phinyocheep, S. Kittipoom, W. Pattanasiriwisawa, Y. Ikeda, *Polym. Adv. Technol.*, 2012, **23**, 1335.

26. A. Tohsan, Y. Ikeda, *Chemistry, manufacture and applications of natural rubber*, ed. S. Kohjiya, Y. Ikeda, Woodhead/Elsevier, Cambridge, 2014, Chapter 6, 168-192.

27. D. C. Blackley, *Polymer Lattices Science and Technology Volume 2*, Chapman & Hall, London, 1997.

28. K. Nawamawat, J. T. Sakdapipanich, C. C. Ho, Y. Ma, J. Song, J. G. Vancsod, *Colloids Surf, A*, 2011, **390**, 157.

29. J. Sakdapipanich, R. Kalah, A. Nimpaiboon, C. C. Ho, *Colloids and Surfaces A: Physicochem. Eng. Aspects*, 2015, **466**, 100.

CHAPTER 3

CHAPTER 3

Strain-Induced Crystallization Behaviours of Lignin/Natural Rubber Soft Biocomposites

3.1 Introduction

The superior mechanical properties of natural rubber (NR) as compared to synthetic rubbers are well understood that they occurs from strain-induced crystallization (SIC) [1-4]. In the other word, the SIC behaviour is ascribable to the non-uniformity of natural network structure in NR, i.e., non-rubber components, as proved by atomic force microscopy and small-angle neutron scattering analyses [5]. The general phenomenon of SIC behaviour in NR is noticed: the crystallites are usually detected to grow up along the direction perpendicular to the molecular chain axis [6,7] and successively occurred upon stretching. Typically, the SIC has been believed to increase modulus, in which the crystallites are considered to bear the tensile stress. Additionally, the SIC behaviour significantly depends on the cross-linking systems, e.g. sulfur or peroxide cross-links, in the other word, the inhomogeneity of cross-linked NR also affects to the SIC behaviour [8].

NR is often reinforced with filler in order to enhance the desired properties, reduce the cost, improve processing, etc. The particle fillers such as carbon black and precipitated silica are importance in tyres manufacturing. The study on the SIC behaviour of NR has been extensively carried out during the last decade [1-3,9,10], not only for cross-linked NR [2,8-10] but also for filler-filled cross-linked NR [6,7,11]. The SIC behaviour of filler-filled cross-linked NR composites, for example, carbon

black/NR composites [11-14], graphene/NR composites [15], and *in situ* silica/NR composites [7,16], has been studied by researchers. They found that the incorporation of these reinforcing fillers affected to the SIC, i.e., the onset of crystallization is significantly detected at smaller strain comparing with the unfilled NR. This means that the SIC is apparently accelerated.

A filler network has been focused from many researchers, because it has been considered to transfer the stress and enhance the mechanical properties effectively [17-23]. However, the network of filler was mostly found at high content of filler loading, for example, a network of carbon black was started to form at around 30 parts per one hundred rubber by weight [23]. Recently, our research group reported the stepwise SIC of *in situ* silica/NR composites with the unique morphology of *in situ* silica network-like structure prepared by the soft process. The NR particles play a role as templates to form biphasic structure in the composites, i.e., the *in situ* silica is locally dispersed around the rubber particles [16]. The results showed that the size distribution of NR particles in latex stage provides this specific SIC behaviour.

Lignin was intensively focused in this study. Lignin is the second most abundant biopolymers next to cellulose, which has many advantageous properties such as reinforcing effect, biodegradability, etc.[24,25] A promising reuse of the lignin waste as an organic filler component in rubbery composites has been carried out extensively [26-28]. According to the outstanding filler network morphology of *in situ* silica/NR composites [16], this leading idea is inspired our research group to prepare the lignin/NR biocomposites by using effective soft process, in which the stepwise SIC is expected to detect. Lately, we successfully prepared lignin/NR soft biocomposite composing network-like filler even only 10 phr of lignin to result in high mechanical

properties [28]. To further investigate the role of network-like structured lignin, the elucidation of SIC behaviour is necessary.

In this study, the role of network-like structure of lignin at different lignin loadings on their SIC behaviours was investigated using the quick time-resolved simultaneous wide-angle X-ray diffraction/tensile measurements. The unique SIC features of the NR soft biocomposites were quantitatively discussed in details for the first time. The effect of network-like structure on SIC behaviour of organic filler "lignin" was predicted to be different from that of *in situ* silica, which was inorganic filler. Thus, the present SIC behaviour of lignin/NR soft biocomposites will be one of keys to reveal the role of network-like filler in the case of organic filler and is probably useful for the development of rubber-based green composites.

3.2. Experimental

3.2.1 Materials

Lignin/natural rubber (lignin/NR) soft biocomposites were prepared by soft processing method from the NR latex. The cross-linked biocomposites films were prepared as followed: High ammonia NR latex of 100 ml was mixed with 50% sulfur dispersion of 1.5 parts per one hundred rubber by weight (phr), 50% ZDEC dispersion of 1.0 phr and 50% ZnO dispersion of 1.8 phr at r.t. in advance, and followed by mixing with the Na-LS aqueous alkaline solutions of 10 and 40 phr lignin. Since Na-LS from kraft process is hydrophobic, it is soluble in organic solvents but is practically insoluble in water [29]. Thus, it is difficult to mix the lignin powder with the NR latex directly. Regarding to the NR latex, it is preserved by NH_4OH basic condition, which is preferable for mixing. Therefore, the Na-LS solution was prepared by stirring in an

aqueous NaOH solution of 0.1 mol/l. The final concentration of lignin solution was 30 w/v%. The biocomposites were prepared by casting the liquid mixture on a glass plate, and they were evaporated at r.t. for a few days. The obtained films were subjected to cross-linking at 70 ^{o}C for 4 h, and were dried at r.t. under a reduced pressure. Note that an unfilled sample was also prepared by the same method. Here after NR-L0-S-soft, NR-L10-S-soft and NR-L40-S-soft was abbreviated for 0, 10 and 40 phr lignin filled NR soft biocomposites. In the sample code, "L", "number" and "S" mean lignin, a content of lignin in phr, and a sulfur cross-linking, respectively.

3.2.2 Morphology observation by scanning probe microscopy

Scanning probe microscopy (SPM) observation was performed using the same machine probes and preparation of surface as described in Chapter 1 section 1.2.4. Here, phase SPM images of NR-L10-S-soft and NR-L40-S-soft are shown in Figure 3.1 with that of NR-L0-S-soft. Bright and dark parts correspond to hard and soft phases, indicating the lignin and the NR phases, respectively, in NR-L10-S-soft and NR-L40-S-soft. The lignin was located around the NR particles in the latex during film forming to result in the selective formation of lignin phases around the rubber phases [28].

3.2.3 Quick time-resolved simultaneous wide-angle X-ray diffraction and tensile measurements

Quick time-resolved simultaneous wide-angle X-ray diffraction (WAXD) and tensile measurements were carried out at BL-40XU in SPring-8, Harima, Japan. A tailor-made tensile machine (ISUT-2201, Aiesu Giken, Co., Kyoto, Japan) was situated

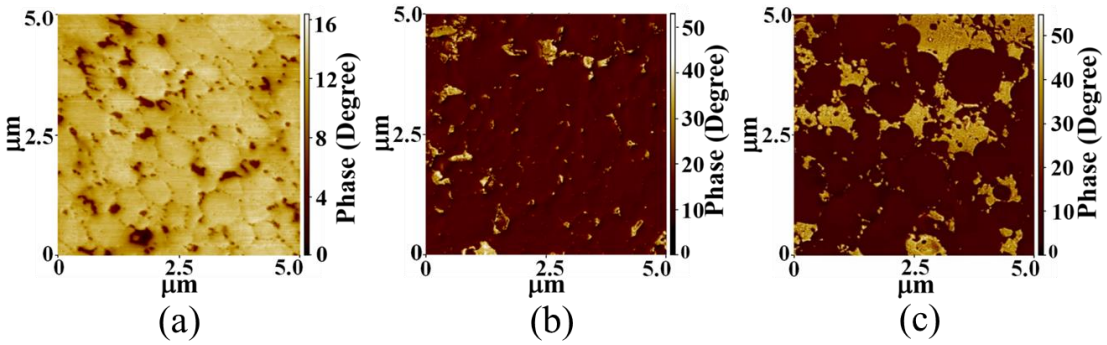

Figure 3.1 SPM phase images of (a) unfilled NR, (b) NR-L10-S-soft and (c) NR-L40-S-soft.

on the beam line, and WAXD patterns were recorded during tensile measurement at r.t. temperature (*ca.* 25 °C). Outside and inside diameters of ring-shaped samples were 13.7 and 11.7 mm, respectively. The ring-shaped samples were stretched up to the rupture point with a stretching speed of 100 mm/min. A stretching ratio (α) is defined as $\alpha = l/l_0$, where α is the stretching ratio, l is a length after deformation, and l_0 is an initial length, respectively. The wavelength of X-ray was 0.08322 nm and the camera length was 184.7 mm. Two-dimensional WAXD patterns were recorded using a charge-coupled device (CCD) camera (ORCA II, Hamamatsu Photonics, Co.). Intensity of the incident X-ray was attenuated using a rotating slit equipped on the beam line, and the incident beam was exposed on the sample for 70 ms every 3 s. An absorption correction for thin sample during deformation was estimated by using the calculation of correction coefficients, which were evaluated on the basis of absorption coefficients per density [8] and weight fractions of each element in the sample. Here, an affine deformation was assumed for all rubber samples on the basis of Poisson's ratios. The Poisson's ratios were measured separately under the similar experimental condition with that of

simultaneous WAXD and tensile measurements using a CCD camera (VC1000 Digital Fine Scope, OMRON Co.). The measured values of Poisson's ratio are 0.487, 0.471 and 0.425 for NR-L0-S-soft, NR-L10-S-soft and NR-L40-S-soft, respectively.

3.2.4 WAXD analysis

The obtained WAXD images were processed using software "POLAR" (Stonybrook Technology & Applied Research, Inc.) [2,10,30]. Each WAXD pattern of extended sample was separated into three components, i.e., isotropic, oriented amorphous and crystalline components. Three components were azimuthally integrated within the range of ±75° from the equator; the details of this analytical method were described in our previous papers [2,10]. Two structural parameters were estimated at first, of which "crystallinity index" (CI) and "oriented amorphous index" (OAI) are defined by the following equations.

$$\mathrm{CI} = \frac{\sum_{crystal} 2\pi \int \sin\phi d\phi \int I(s)s^2 ds}{\sum_{total} 2\pi \int \sin\phi d\phi \int I(s)s^2 ds} \quad (1)$$

$$\mathrm{OAI} = \frac{\sum_{oriented\ amorphous} 2\pi \int \sin\phi d\phi \int I(s)s^2 ds}{\sum_{total} 2\pi \int \sin\phi d\phi \int I(s)s^2 ds} \quad (2)$$

By summation of CI and OAI, the oriented index (OI) can be obtained as showed in eqn (3);

$$OI = CI + OAI \quad (3)$$

In eqn (1) and (2), *I(s)* represents the intensity distribution of each peak that is read out from the WAXD pattern, *s* is the radial coordinate in reciprocal space in nm^{-1} unit ($s = 2(\sin \theta/\lambda)$, where λ is the wavelength and 2θ is the scattering angle), and ϕ is the angle between the scattering vector of the peak and the fiber direction.

Coherent lengths (apparent crystallite sizes) were estimated by using the Scherrer equation (eqn (4)); [31]

$$L_{hkl} = K\lambda/(\beta \cos \theta) \quad (4)$$

where L_{hkl} is the apparent crystallite size in the direction perpendicular to the (hkl) plane, λ is the wavelength, and θ is the Bragg angle (half of the scattering angle). In this study, the value 0.89 was used for *K* [32]. The intensity distribution on the equator was extracted from the original WAXD pattern. Each peak was fitted with a linear background and a Gaussian function having the form $I(x) = h \exp[-(x-x_c)^2/(2w^2)]$, where *I(x)* is the intensity at position (*x*), x_c is the position at the scattering maximum, and *h* and *w* are parameters related to the peak height and the peak width, respectively [2,10]. Each of *w* value was converted into the half-width (β).

Orientation fluctuations of 200 reflection were evaluated from azimuthal scan of the peak. The width parameter in azimuthal direction (w_{az}) was obtained by fitting the intensity distribution with a Gaussian function. Then w_{az} was converted into half-width β_{az} by the following equation;

$$\beta_{az} = 2w_{az}\sqrt{-2\ln(1/2)} \tag{5}$$

Lattice constants (*a*, *b* and *c*) were estimated from the WAXD patterns obtained during the deformation process using the least-squares regression method [2].

Furthermore, the average volume of the crystallites (V_c) was evaluated by using the equation as follow. It was reported that the angle α between the (120) and the (020) directions is *ca.* 19°, thus the value of L_{020} is approximated as $0.94L_{120}$ [33]. This reported angle is very similar to the estimated angle by the value of lattice constant in our experimental data.

$$V_c = L_{200}L_{020}L_{002} = 0.94L_{200}L_{120}L_{002} \tag{6}$$

Assuming that crystallites have identical dimensions at a given stretching ratio, an average number of the crystallites per unit volume can be calculated using the V_c [33]. However, the CI value in this study was the crystallinity index. Therefore, the index of average number of the crystallites per unit volume (*N*) was calculated using eqn (7); [34]

$$N = \frac{\mathrm{CI}}{V_c} \tag{7}$$

3.3 Results and discussion

3.3.1 Characteristic of strain-generated crystallites in lignin/NR soft biocomposites

Considering the unique morphologies of 10 phr and 40 phr lignin filled NR soft biocomposites (NR-L10-S-soft and NR-L40-S-soft, respectively) with their unfilled sample (NR-L0-S-soft) as revealed in Figure 3.1, the interphase between the rubber phases (the beige phases) in unfilled sample became harder after adding 10 and 40 phr of lignin. This phenomenon clearly suggests that the lignin plays a role to reinforce at the interphase, where the sodium lignosulfonate containing ionic sites has a good interaction with the non-rubber components. Note that the lignin phase became larger when the amount of lignin was reached to 40 phr. This means that NR-L40-S-soft not only composed the efficient filler-rubber interaction at the interphase, but also contained the higher lignin-lignin interaction compared to NR-L10-S-soft. The presence of filler-rubber interaction only at the interphase of NR-L10-S-soft and NR-L40-S-soft was confirmed as an identical glass transition temperature (T_g) of pure rubber phase determined by the dynamic mechanical analysis (DMA). Also, the stronger Payne effect of NR-L40-S-soft than NR-L10-S-soft suggested the significantly higher filler-filler interaction in the former than the latter. The Payne effect and DMA results were shown in previous chapter (Figure 2.6 and 2.7, respectively). The different morphological features between these two NR soft biocomposites were predicted to be a key factor affecting their reinforcement mechanisms and properties. Figure 3.2 shows the tensile stress–strain curves up to mechanical rupture points of NR-L10-S-soft and NR-L40-S-soft with that of NR-L0-S-soft. The considerable tensile stress upturn at large strain was found in NR-L10-S-soft similarly to that in NR-L0-S-soft, and the upturning degree of the former was larger than the latter. The stress of NR-L40-S-soft

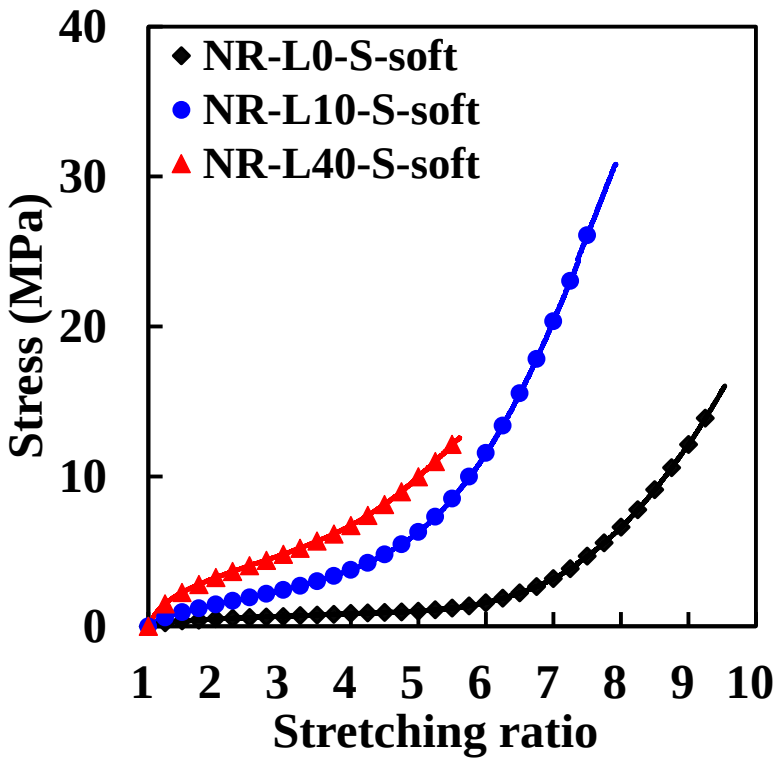

Figure 3.2 Tensile stress-strain curves of lignin/NR soft biocomposites and unfilled NR.

significantly increased from the low strain, indicating the presence of strong filler-filler interaction. However, it did not show much abrupt stress upturn at large strain. From the basis of their unique morphologies, the reinforcement mechanisms of the NR soft biocomposites were found to be different at 10 and 40 phr of lignin filling.

It has been reported that the strain-induced crystallization (SIC) has much influence on tensile properties of NR at large deformation [2,8,10]. Therefore, we speculated that a strengthened lignin/rubber interphase with less restricted lignin network-like structure in NR-L10-S-soft promoted the SIC of the NR soft biocomposite, resulting in the significant higher degree of stress upturn at large strain. On the other hand, the

strengthened interphase with the highly stiff lignin network-like structure in NR-L40-S-soft probably prevented the SIC behaviour but reinforced the biocomposite, leading to the substantially improved stress without the upturn at large strain. Based on these speculations, the SIC behaviours of NR-L10-S-soft and NR-L40-S-soft with their unfilled sample detected by the simultaneous time-resolved WAXD and tensile measurements were quantitatively determined and deeply discussed in this chapter.

The variation of SIC parameters, i.e., oriented index (OI), oriented amorphous index (OAI) and crystallinity index (CI) of the NR soft biocomposites and the unfilled NR against stretching ratios are shown in Figure 3.3. NR-L10-S-soft and NR-L40-S-soft showed the increase of OI with increasing stretching ratio as similarly observed in the unfilled sample. Both biocomposites exhibited the considerably higher OI than the unfilled sample at all stretching ratios. This suggests that the orientation of NR molecular chains was increased by the addition of lignin. It may be because the high filler-rubber interaction at the interphases of NR-L10-S-soft and NR-L40-S-soft promotes the orientation of rubber chains inside the rubber phases. In addition, the OI of NR-L40-S-soft was lower than that of NR-L10-S-soft at low strain and then their OI values became similar after $\alpha \geq 2.75$ as presented in Figure 3.3(a). That means, at a low deformation, the rubber chain orientation in NR-L40-S-soft seemed to be strongly restricted by the highly stiff lignin network-like structure. Even though the orientation becomes better with further stretching due to the breakage of some filler-filler interactions, it did not much improve when compared to 10 phr lignin filling sample. These features were much clearly observed in the OAI results of the NR soft biocomposites and the unfilled sample with the higher fluctuated changing against stretching ratio as can be seen in Figure 3.3(b). Interestingly, the variation of OAI

against stretching ratios for NR-L10-S-soft and NR-L0-S-soft provided two distinct steps. First, NR-L10-S-soft and NR-L0-S-soft showed the plateau regions in the range of $1.5 \leq \alpha \leq 4.75$ and $1.5 \leq \alpha \leq 5.75$, respectively. This is because the large deformation of rubber chains in the small rubber phases and starting deformation in big rubber phases were compensated. Second step was the gradually increased OAI until near the rupture points in both samples. In this region, the major rubber orientation was probably occurred in the big rubber phases. Two steps of OAI results agreed well with the plateau region at low deformation with a high stress upturn at large deformation in the stress-strain curves of NR-L10-S-soft and NR-L0-S-soft. On the other hand, the OAI of NR-L40-S-soft continuously increased with increasing stretching ratio without a plateau region of OAI. This also corresponds to the absence of plateau region in the stress-strain curve of NR-L40-S-soft. These results bring about the assumption that the oriented amorphous components in each NR soft biocomposite are probably one of the important roles to give an enhancement of tensile stress.

In vulcanized rubber, the strain-induced crystallites are supposed to be sufficiently connected to the oriented amorphous rubber chains, to load the applied force at larger deformations. Thus, the difference of tensile stress among the samples at large strain is more clearly understood by relating these differences to the SIC phenomena. Figure 3.3(c) shows the variation of CI for NR-L10-S-soft and NR-L40-S-soft plotted against stretching ratio with that of NR-L0-S-soft. Unexpectedly, the CI values were similar among the samples. Therefore, till now, we can conclude that the crystalline phases in NR-L10-S-soft did not much contribute to load the applied stress, but the main players for the substantial enhancement of its stress are the large amount of oriented amorphous components and direct reinforcement of lignin. These results are the good answer for

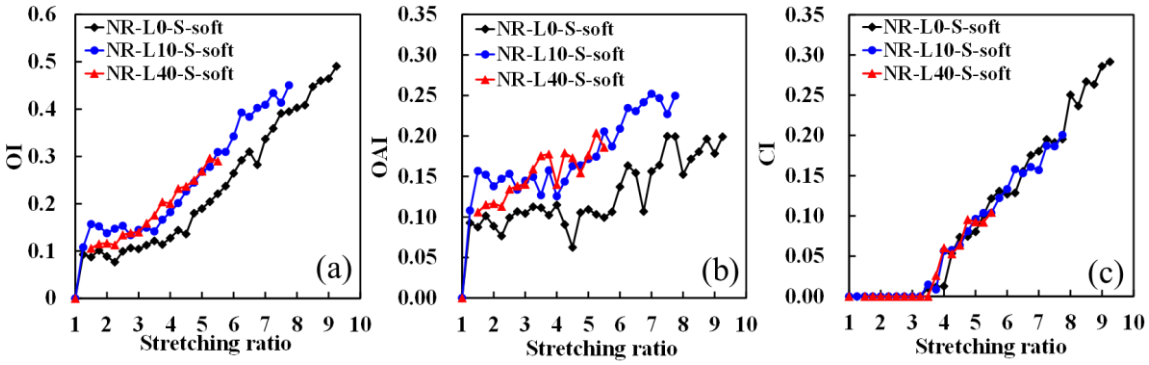

Figure 3.3 Variations of (a) OI, (b) OAI and (c) CI for lignin/NR soft biocomposites and unfilled NR plotted against the stretching ratio.

our speculations as mentioned before. The efficient filler-rubber interaction in NR-L10-S-soft mainly promotes the orientation of NR chains in the rubber phase along the stretching direction, but prevents the further development of crystalline phases.

Additionally, the presence of randomly dispersed lignin aggregates after network-like filler breakage seemed to disturb the development of crystallites as well. Moreover, the similar CI and OAI of NR-L40-S-soft to those of NR-L10-S-soft at large strain confirm the occurrence of same phenomena in these two samples, which are principally attributed to the filler-rubber interaction. The filler morphologies in the composites seemed not to affect the development of crystallites. As a result, it can be said that the improvement of tensile stress for the NR-L40-S-soft is mainly resulted from the lignin reinforcement.

Besides, the CI of all the samples did not linearly increase with increasing stretching ratio, but they exhibited the stepwise phenomenon, consisting of plateau region and small increase of CI during upward change. Note that the small plateau regions of the CI values were repeatedly detected. The onset strain of SIC (α_c) for NR-L10-S-soft was

same as that of NR-L0-S-soft, which was at $\alpha = 3.5$. However, NR-L40-S-soft showed the slightly larger α_c at 3.75 with the missing of first step. This result suggests that the highly stiff network-like structure of lignin at 40 phr delays the onset strain of SIC, and supposed to prevent the SIC of small sized NR phases for NR-L40-S-soft. This phenomenon is different from the other previous reports on the SIC behaviour of the composites, i.e., the α_c of filler filled composites becomes earlier with increasing of filler contents [11,16]. The SIC characteristic observed in this study was revealed for the first time to the best of our knowledge.

The stepwise SIC behaviours are supposed to be due to the unique biphasic structure in the composites prepared by the soft processing method [16]. Some differences in stepwise SIC of the lignin/NR soft biocomposites and the unfilled NR were found when each step was considered carefully. The strain required for each step in NR-L10-S-soft was similar to that of NR-L40-S-soft, but it seemed to be smaller than that of unfilled sample. This phenomenon is accelerated by the strengthened interphase of NR soft biocomposites. However, notably, each CI step tended to become flatter with the increase of lignin content. This refers that the rate of crystallization in each step may be disturbed by the presence of higher lignin content.

In the case of organic filler, lignin, this unique stepwise SIC was observed similarly to our previous results on *in situ* silica filled NR composite [16]. In this study, the role of filler morphology and filler-rubber interaction on the SIC behaviour of NR composites prepared by soft processing could be extensively explained from the previous results. That is, the further development of crystallites at high strain was controlled by the filler-rubber interaction, not depending on the filler morphology. By using the soft processing technique, these two important factors on the properties of NR

composites can be separately considered here. As previously reported, the characteristics of generated strain-induced crystallites, e.g. size, volume and number of crystallites also have an influence on the large deformation behaviour of rubbers [34]. Therefore, the other SIC parameters for generated crystallites are quantitatively discussed in the next section.

Apparent crystallite sizes (coherent lengths) during stretching were determined from the WAXD profiles by the Scherrer equation [31]. The calculated coherent lengths are reasonably assumed to reflect actual crystallite sizes. Figure 3.4(a), (b) and (c) show the strain dependences of apparent lateral crystallite sizes for the lignin/NR biocomposites and the unfilled NR estimated by using the 200 (L_{200}), 120 (L_{120}) and 002 (L_{002}) reflections, respectively. The apparent crystallite sizes in 200, 120 and 002 reflections for all the samples decreased with increasing stretching ratio. Both NR soft biocomposites showed the smaller apparent crystallite sizes in all reflection planes than the unfilled sample at a particular stretching ratio. Moreover, it has no significant difference in apparent crystallite sizes, i.e., L_{200}, L_{120} and L_{002} between NR-L10-S-soft and NR-L40-S-soft when the error standard deviation was regarded. This means that the development of crystallites size was more perturbed with the presence of lignin, but not related to the different filler morphologies. The filler-rubber interaction seemed to be only one factor most controlling this behaviour. Using the parameters of CI and three apparent lateral crystallite sizes, volumes of generated crystallites were calculated and compared among the samples. Due to the reduction of apparent crystallite size upon stretching for all the samples, their average crystallite volume (V_c) values tended to decrease with increasing stretching ratio as shown in Figure 3.4(d). As expected, the V_c of the lignin/NR soft biocomposites was significantly smaller than that of the unfilled

sample at a given stretching ratio, and the V_c of NR-L40-S-soft was not much different from that of NR-L10-S-soft. On the other hand, the average numbers of crystallite per unit volume (N) of both composites increased with increasing stretching ratio similarly to those observed in the unfilled sample as can be seen in Figure 3.4(e). The N values were comparable between NR-L10-S-soft and NR-L40-S-soft, but they were much higher than that of NR-L0-S-soft. This may be because the interaction between the lignin and the rubber phases can act as the additional starting sites to generate the more crystallites. Till now, we can conclude that the similar CI of both NR soft biocomposites with the unfilled sample is due to the competitive effect of smaller crystallite volume but larger number of crystallites for the composites. For the rubber science and technology, the smaller the filler size, the stronger the reinforcement effect is. In addition, it has been thought that generated crystallites can act as the reinforcing filler for the rubber matrix. Therefore, the smaller crystallite size and larger number of crystallites of NR soft biocomposites than the unfilled sample may give the advantages for the reinforcing efficiency of SIC in this study. Additionally, of course, the influence of orientation of crystallites during stretching should be taken into account to explain the development of strain-generated crystallites.

Figure 3.4(f) shows the strain dependence of orientation fluctuation of crystallites (β_{az}) for the lignin/NR soft biocomposites and the unfilled NR. Here, the smaller value of β_{az} means the smaller fluctuations in orientation. As shown in the Figure 3.4(f), the β_{az} values of the NR soft biocomposites decreased with increase of lignin content. However, the degree of decreasing β_{az} against stretching ratio was larger in the composites than the unfilled NR. This means that the presence of lignin, especially the

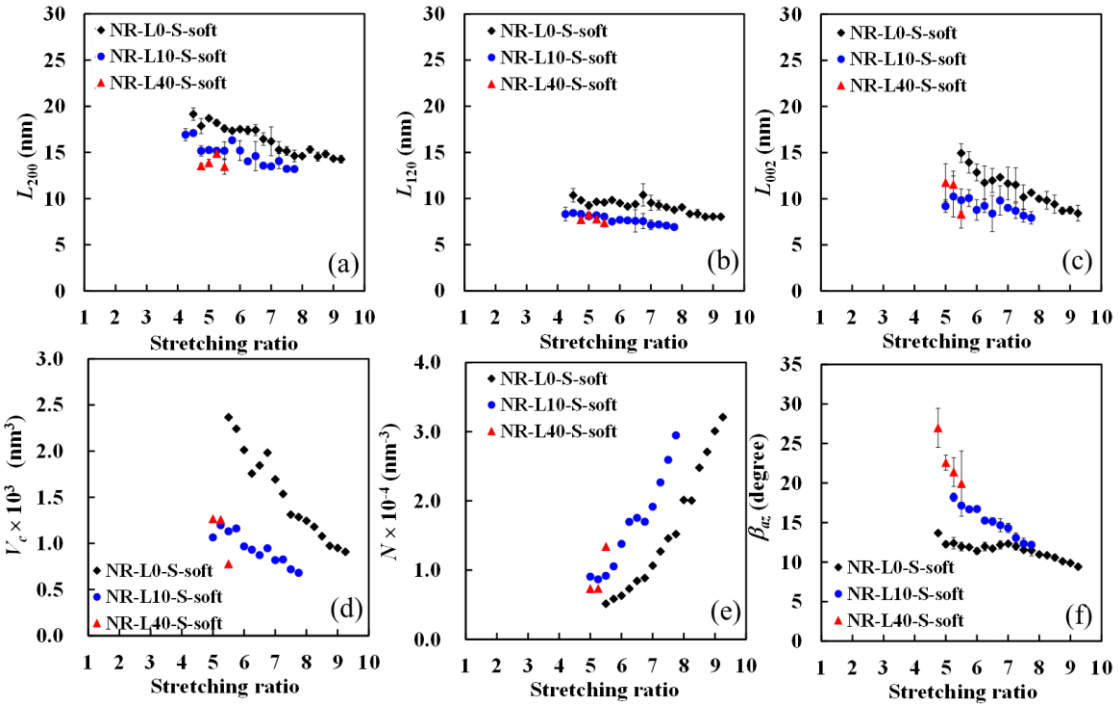

Figure 3.4 Variations of apparent crystallite sizes: (a) $L_{200,}$ (b) L_{120} and (c) L_{002}, and variation of (d) average crystallite volume, (e) indexes of average number of crystallites per unit volume and (f) orientationl fluctuation of crystallites for lignin/NR soft biocomposites and unfilled NR plotted against the stretching ratio.

large lignin-lignin phase in NR-L40-S-soft, disturbed the orientation of crystallite along the stretching direction. The fluctuation degree of β_{az} for all the samples decreased with further stretching. This is probably due to the depression of fluctuated crystallites orientation by the decrease of crystallites sizes at larger strain. The large orientation fluctuation of crystallite in NR soft biocomposites is one of the reasons for the low stress transfer efficiency of SIC even they have small crystallite sizes and large crystallite number. In order to reveal the effect of SIC behaviour on the tensile properties more clearly, the variation of SIC parameters, i.e., OI, OAI and CI against

stress has to be considered.

3.3.2 Relationship between tensile properties and SIC behaviors of lignin/NR soft biocomposites

The stress dependence of OI, OAI and CI is also clearly observed in Figure 3.5(a)-(c), respectively. At a particular stress, it appears that the OI values were higher in an order of NR-L40-S-soft, NR-L10-S-soft and NR-L0-S-soft, respectively. Moreover, the OAI values of NR-L10-S-soft and NR-L0-S-soft were higher than those of NR-L40-S-soft at the stress ≤ 5 MPa. This confirms that the stress prefers to be transferred by filler-filler networks in NR-L40-S-soft than oriented amorphous segments at low deformation. After the stress was higher than 5 MPa, NR-L10-S-soft gave the larger OAI, and NR-L40-S-soft generated the comparable OAI compared to those of unfilled sample due to the breakage of some filler-filler interactions. NR-L10-S-soft having the smaller filler-filler interaction needs the larger oriented

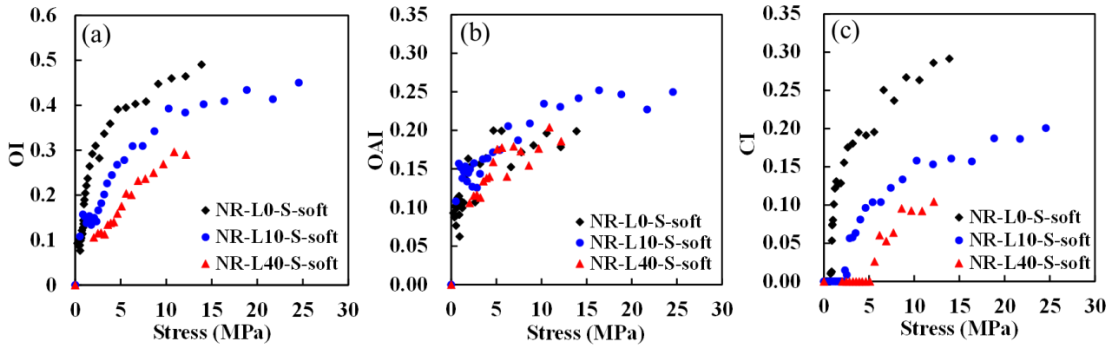

Figure 3.5 Variations of (a) OI, (b) OAI and (c) CI for lignin/NR soft biocomposites and unfilled NR plotted against the nominal stress.

amorphous segments than NR-L40-S-soft to support the lignin reinforcement. The lower CI values of NR-L10-S-soft and NR-L40-S-soft than NR-L0-S-soft at the same stress also affirm that the main important roles to transfer the stress are the network-like structure of lignin and oriented amorphous segments. Additionally, the deformation of crystal lattice by the stress upon stretching is shown in Figure 3.6. The lattice constants were estimated from the WAXD patterns during deformation by using the least-square regression method. The unit cell was assumed to be a rectangular which proposed by Nyburg [36]. The unit cell contracts along *a* and *b* directions (perpendicular to the stretching direction) and elongates in the *c* direction (parallel to the stretching direction).

Even though the strain-induced crystallites are not the main factor for an enhancement of tensile stress in the NR soft biocomposites, they still partially supported the stress confirmed as an almost linear relationship of the unit cell with the stress for all the samples. The lattice constants in *a* and *b* directions of lignin/NR soft biocomposites were slightly larger than those of unfilled NR at a particular stress, but

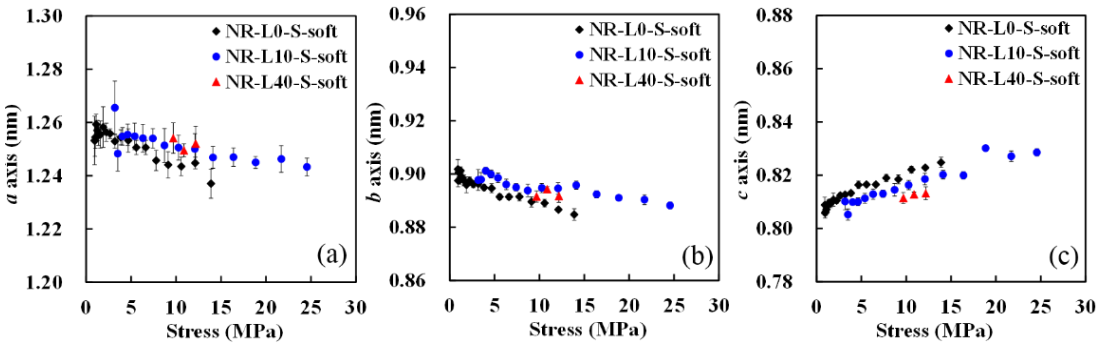

Figure 3.6 Variation of lattice constants in; (a) *a* axis, (b) *b* axis, (c) *c* axis of lignin/NR soft biocomposites and unfilled NR plotted against the nominal stress.

the lattice constant in *c* direction of the former was smaller than the latter. This confirmed that the deformation of unit cell along the stretching direction for the lignin/NR soft biocomposites was smaller when compared to NR-L0-S-soft. Moreover, the less steep slope of lattice constants against stress for NR-L10-S-soft than NR-L0-S-soft suggested that the almost stress were not directly loaded by strain-induced crystallites but by oriented amorphous segments and network-like structure of lignin.

3.4 Conclusions

The quick time-resolved simultaneous wide-angle X-ray diffraction/tensile measurements during stretching revealed the strain-induced crystallization (SIC) behaviour of the high performance lignin/NR soft biocomposites. The behaviour found in the composites directly prepared from NR latex with lignin using soft processing method. The size distribution of rubber particles in NR latex accelerated the stepwise SIC even different lignin contents were loaded, i.e., 10 and 40 phr. Both NR biocomposites provided the comparable oriented amorphous components at large strain and similar crystallinity. The higher filler-rubber interaction at the interphase of the composites was considered as a key factor to orient the NR molecular chain in the rubber phases, however, the further development of crystallites was prevented. Moreover, the higher filler-filler interaction of 40 phr filled NR bicomposites was not found to be much different on its SIC behaviour comparing with those of 10 phr filled NR biocomposites. For example, it exhibited the comparable apparent crystallite sizes and volume including number of crystallites to the 10 phr lignin filling ones. It is assure that the filler morphology of the NR soft bicomposites has no influence on the

development of crystallites at large strain. However, the higher filler-filler interaction of 40 phr lignin filling sample delayed the onset SIC and retard the crystallization rate in each SIC step but provided the larger orientation fluctuation of crystallites along the stretching direction, compared to 10 phr of lignin filled NR soft biocomposite and unfilled NR, respectively. Additionally, the stress dependence of SIC results can be confirmed that the oriented amorphous components supported the lignin network-like structure in the NR soft biocomposites to load stress. This is interesting that the role of filler network for an enhancement of the tensile stress of NR soft biocomposites could be deeply understood from the viewpoint of organic biofiller "Lignin". The effects of filler-rubber interaction and filler morphology on the SIC behaviours were clearly separately discussed in this study. It may note to be useful in progress for the preparation and development of high performance sustainable composites.

References

1. S. Toki, I. Sics, S. Ran, L. Liu, B. S. Hsiao, S. Murakami, K. Senoo, S. Kohjiya, *Macromolecules*, 2002, **35**, 6578.

2. M. Tosaka, S. Murakami, S. Poompradub, S. Kohjiya, Y. Ikeda, S. Toki, I. Sics, B. S. Hsiao, *Macromolecules*, 2004, **37**, 3299.

3. S. Murakami, Senoo K., Toki S., Kohjiya S., *Polymer*, **2002**, 43, 2117.

4. P. J. Flory, *J. Chem. Phys.*, 1947, **15**, 397.

5. T. Karino, Y. Ikeda, Y. Yasuda, S. Kohjiya, Shibayama M., *Biomacromolecules*, 2007, **8**, 693.

6. Y. Ikeda, A. Kato, J. Shimanuki, S. Kohjiya, M. Tosaka, S. Poompradub, S. Toki, B. S. Hsiao, *Rubber Chem. Technol.*, 2007, **80**, 251.

7. Y. Ikeda, *Kautsch. Gummi. Kunstst.*, 2005, **58**, 455.

8. Y. Ikeda, Y. Yasuda, K. Hijikata, M. Tosaka, S. Kohjiya, *Macromolecules*, 2008, **41**, 5876.

9. Y. Ikeda, Y. Yasuda, S. Makino, S. Yamamoto, M. Tosaka, K. Senoo, S. Kohjiya, *Polymer*, 2007, **48**, 1171.

10. M. Tosaka, S. Kohjiya, S. Murakami, S. Poompradub, Y. Ikeda, S. Toki, I. Sics, B. S. Hsiao, *Rubber Chem. Technol.*, 2004, **77**, 711.

11. S. Poompradub, M. Tosaka, S. Kohjiya, Y. Ikeda, S. Toki, I. Sics, B. S. Hsiao, *J. Appl. Phys.*, 2005, **97**, 103529/1.

12. S. D. Gehman, J. E. Field, *Rubber Chem. Technol.*, 1941, **14**, 85.

13. S. Trabelsi, P. A. Albouy, *Macromolecules*, 2003, **36**, 9093.

14. S. Dupres, D. R. Long, P. A. Albouy, A. Sotta, *Macromolecules*, 2009, **42**, 2634.

15. B. Ozbas, S. Toki, B. S. Hsiao, B. Chu, R. A. Register, I. A. Aksay, R. K. Prud′homme, D. H. Adamson, *J. Polym. Sci., Part B: Polym. Phys.*, 2012, **50**, 718.

16. Y. Ikeda, A. Tohsan, *Colloid Polym. Sci.*, 2014, **292**, 567.

17. F. Bueche, *Reinforcement of elastomers*, ed G. Kraus**,** Interscience, New York, 1965, Chapter 1, 1.

18. M. Klüppel, *Adv. Polym. Sci*., 2003, **164**, 1.

19. S. Kohjiya, A. Kato, T. Suda, J. Shimanuki, Y. Ikeda, *Polymer*, 2006, **47**, 3298.

20. S. Kohjiya, A. Kato, Y. Ikeda, *Prog. Polym. Sci.*, 2008, **33**, 979.

21. F. Deng, M. Ito, T. Noguchi, Y. A. Kim, M. Endo, Q. S. Zheng, *ACS Nano*, 2011, **5**, 3858.

22. A. Tohsan, R. Kishi, Y. Ikeda, *Colloid Polym. Sci.*, 2015, **293**, 2083.

23. L. Chen, L. Song, J. Li, P. Chen, N. Huang, L. B. Li, *Macromol. Mater. Eng.*, 2016,

301, 1390.

24. M. A. De Paoli, L. T. Furlan, *Polym. Degrad. Stab.***,** 1985, **11**, 327.

25. C. G. Boeriu, D. Bravo, R. J. A. Gosselink and J. E. G. van Dam, *Ind. Crops Products*, 2004, **20**, 205.

26. V. K. Thakur, M. K. Thakur, P. Raghavan, M. R. Kessler, *ACS Sustainable Chem. Eng.*, 2014, **2,** 1072.

27. E. Ten, W. Vermerris, *J. Appl. Polym. Sci.*, 2015, 42069(1).

28. T. Phakkeeree, Y. Ikeda, H. Yokohama, R. Kitano, A. Kato, *J. Fiber Sci. Technol.*, 2016, **72**, 160.

29. H. Chung, N.R. Washburn, *Green Mater.*, 2012, **1**, 137.

30. S. Trabelsi, P.A. Albouy, J. Rault, *Macromolecules*, 2002, **35**, 10054.

31. P. Scherrer, *Gottinger. Nachrichten.*, 1918, **2**, 96.

32. H. P. Klug, L. E. Alexander, *X-ray diffraction procedures for polycrystalline and amorphous materials*, 2nd ed, Wiley-Interscience, New York, 1974.

33. N. Candau, R. Laghmach, L. Chazeau, J. M. Chenal, C. Gauthier, T. Biben, E. Munch, *Macromolecules*, 2014, **47**, 5815.

34. Y. Ikeda, P. Junkong, T. Ohashi, T. Phakkeeree, Y. Sakaki, A. Tohsan, S. Kohjiya, K. Cornish, *RSC Adv.*, 2016, **6**, 95601.

35. L. R. G. Treloar, *The physics of rubber elasticity*, Clarendon Press, Oxford, 1975.

36. S. C. Nyburg, *Acta Crystallogr.*, 1954, **7**, 385.

SUMMARY

The lignin as a waste from paper-pulping manufacture was successful of use as an effective reinforcing filler in natural rubber (NR) matrix *via* the soft processing method. The effect of reinforcement of lignin for lignin/ NR soft biocomposites was characterized through this study. The contents of respective chapters are summarized as following.

In Chapter 1, the relationship between morphology and mechanical properties of the lignin/NR biocomposite prepared by the soft processing method was revealed. The soft processing method provided not only a good dispersion of lignin in rubbery matrix which can be observed by LSCM analysis, but also a unique formation of network-like structure of lignin which was detected by TEM and SPM analyses. These morphological features analyses revealed that the lignin was locally dispersed around NR phases during film forming. In the other word, rubber particles in the NR latex can play a role as the templates to form the network-like structure of lignin. Thus, the lignin/NR soft biocomposite with network of filler showed the higher mechanical properties even only 10 parts per one hundred rubber by weight (phr) of lignin was added, when compared to the composites prepared by a conventional mixing method at same loading.

In Chapter 2, according to the results in previous chapter, the effect of lignin contents on mechanical properties of lignin/NR soft biocomposites was further studied. The NR biocomposites with various sodium lignosulfonates contents, i.e., 5, 10, 20 and 40 phr, were successfully prepared *via* the soft processing method. As mentioned above, the rubber particles in the NR latex acted as the templates for the formation of locally dispersed lignin around the rubber phases. This phenomenon was still detected even at

the high lignin loading. The presence of a stiff network-like structure of lignin with a high filler-filler interaction in the NR matrix was revealed by the Payne effect. Based on the difference of the unique morphology in lignin filled NR biocomposites, the higher content of lignin in biocomposite provided the more excellent mechanical properties such as substantially higher tensile stresses, larger storage moduli and lower dissipative loss than the lower content of lignin filled biocomposite. However, the low glass transition temperature due to the pure rubber phases was observed similarly in all the biocomposites. This phenomenon is one of significant characteristics of the lignin filled NR biocomposites prepared by the soft processing method.

In Chapter 3, the characteristics of lignin/NR soft biocomposites were announced more by the strain-induced crystallization (SIC). The SIC behaviour of lignin/NR soft biocomposites was elucidated by using a quick time-resolved simultaneous wide-angle X-ray diffraction (WAXD) and tensile measurements. The obtained results revealed the relationship between characteristics of unique morphology and tensile stress-strain properties affiliated with SIC behaviour of the high performance lignin/NR soft biocomposites during stretching. It can be suggested that the significant SIC behaviour was detected in the lignin/NR soft biocomposites, which were directly prepared from NR latex with lignin using the soft processing method. The stepwise SIC was similar among the samples, which is suggested that the size distribution of rubber particles in NR latex was comparable even the different lignin contents were loaded, i.e., 10 and 40 phr. Both lignin/NR biocomposites provided the comparable oriented amorphous components at large strain and similar crystallinity. The high filler-rubber interaction at the interphase of the composites was considered as a key factor to orient the NR molecular chain in the rubber phases, however, the further development of crystallites

was prevented. In addition, the high filler-filler interaction was not found to be much effect on its SIC behaviour. For example, it exhibited the comparable apparent crystallite sizes and volume including number of crystallites to lower lignin filled ones. It undoubted that the filler morphology in the NR soft biocomposites has no influence on the development of crystallites at large strain. However, the high filler-filler interaction delayed the onset SIC and retard the crystallization rate in each SIC step. The oriented amorphous components supported the lignin network-like structure in the NR soft biocomposites to load stress. The role of filler network for an enhancement of the tensile stress of NR soft biocomposites was revealed from the viewpoint of organic biofiller “Lignin”. Thus, it may note to be useful in progress for the preparation and development of high performance sustainable composites.

According to these three chapters in this thesis, the soft processing method was found to be the advantageous method to prepare lignin/NR soft biocomposites with an effective reinforcement of lignin. The results will be useful for developing the already promising reuse of lignin as reinforcing filler for high performance green natural rubber nanocomposites for not only rubber material science but also a sustainable society. In addition, the new lignin filled natural rubber bionanocomposites were found to become adequate models to reveal the reinforcing effect of filler network, which has been one of the important questions for a long time in the field of rubber science and technology. Especially, a role of filler network on the strain-induced crystallization behaviour of the high performance lignin filled natural rubber bionanocomposites was clearly detected in this study.

LIST OF PUBLICATIONS

1. A. Kato, A. Tohsan, S. Kohjiya, T. Phakkeeree, P. Phinyocheep, Y. Ikeda, in "*Progress in Rubber Nanocomposites*", eds. S. Thomas, H. J. Maria, Woodhead Publishing, Oxford, 2016, Chapter 12, 415-461.

(General Introduction, Chapter 1)

2. T. Phakkeeree, Y. Ikeda, H. Yokohama, P. Phinyocheep, R.Kitano, A. Kato, Network-like structure of lignin in natural rubber matrix to form high performance elastomeric bio-composite, *J. Fiber Sci. Technol.*, 2016, **72,** 160.

(Chapter 1)

3. Y. Ikeda, T. Phakkeeree, P. Junkong, H. Yokohama, P. Phinyocheep, R. Kitano, A. Kato, Reinforcing biofiller "lignin" for high performance green natural rubber nanocomposites, RSC Advances, 2017, 7, 5222 - 5231.

(Chapter 2)

4. Y. Ikeda, T. Phakkeeree, P. Junkong, T. Ohashi, Strain-induced crystallization behaviours of lignin/natural rubber soft biocomposites revealed by quick time-resolved simultaneous wide–angle X-ray diffraction, in preparation to be submitted to an international academic journal.

(Chapter 3)

ACKNOWLEDGEMENTS

The author wishes to express her profound gratitude and sincere appreciation to Japanese Government (Monbukagakusho: MEXT) Scholarship for financial support given in undertaking this study.

The author would like to express her sincere gratitude and deep appreciation to the supervisor, Prof. Dr. Yuko Ikeda, for her excellent supervision, fruitful guidance, valuable discussion and kind encouragement throughout this course at Kyoto Institute of Technology.

The author is deeply grateful to Prof. Dr. Shinzo Kohjiya, Professor emeritus of Kyoto University, for giving her an opportunity to become a student in this research group at Kyoto Institute of Technology and his fruitful comments on her study.

The author would like to express her appreciation and thanks to Assoc. Prof. Dr. Pranee Phinyocheep at Department of Chemistry, Mahidol University, for giving her an opportunity to study at Kyoto Institute of Technology.

Her appreciation also goes to all staffs in the International Affair Office and her all colleagues in Soft Materials Research Group at Kyoto Institute of technology, whose names are not mentioned here, for their kind help and support in various ways.

Finally, the author would like to express her thanks to her family for loves, entirely care, encouragement, inspiration and moral support her throughout the course of this study in Kyoto.

December 2016

PHAKKEEREE TREETHIP